

Published in final edited form as:

Eur J Pharm Biopharm. 2014 October ; 88(2): 539–550. doi:10.1016/j.ejpb.2014.07.001.

The effect of co-delivery of paclitaxel and curcumin by transferrin-targeted PEG-PE-based mixed micelles on resistant ovarian cancer in 3-D spheroids and in vivo tumors

Can Sarisozen, Abraham H. Abouzeid, and Vladimir P. Torchilin*

Center for Pharmaceutical Biotechnology and Nanomedicine, Northeastern University, Boston, MA, 02115, USA

Abstract

Multicellular 3D cancer cell culture (spheroids) resemble to in vivo tumors in terms of shape, cell morphology, growth kinetics, gene expression and drug response. However, these characteristics cause very limited drug penetration into deeper parts of the spheroids. In this study, we used multi drug resistant (MDR) ovarian cancer cell spheroid and in vivo tumor models to evaluate the co-delivery of paclitaxel (PCL) and a potent NF- κ B inhibitor curcumin (CUR). PCL and CUR were co-loaded into the polyethylene glycol-phosphatidyl ethanolamine (PEG-PE) based polymeric micelles modified with Transferrin (TF) as the targeting ligand. Cytotoxicity, cellular association and accumulation into the deeper layers were investigated in the spheroids and compared with the monolayer cell culture. Comparing to non-targeted micelles, flow cytometry and confocal imaging proved significantly deeper and higher micelle penetration into the spheroids with TF-targeting. Both in monolayers and spheroids, PCL cytotoxicity was significantly increased when co-delivered with CUR in non-targeted micelles or as single agent in TF-targeted micelles, whereas TF-modification of co-loaded micelles did not further enhance the cytotoxicity. In vivo tumor inhibition studies showed good correlation with the 3D cell culture experiments, which suggests the current spheroid model can be used as an intermediate model for evaluation of co-delivery of anticancer compounds in targeted micelles.

Keywords

Cancer cell spheroids; Multi drug resistance; Paclitaxel; Curcumin; Micelles; Co-delivery; Transferrin

2014 Elsevier B.V. All rights reserved.

***Corresponding Author:** Vladimir P. Torchilin, Ph.D., D. Sc., Distinguished Professor, Northeastern University, Center for Pharmaceutical Biotechnology and Nanomedicine, 140 The Fenway, Room 211/214, 360 Huntington Avenue, Boston, MA 02115, v.torchilin@neu.edu, Phone: 617-373-3206, Fax: 617-373-8886.

Publisher's Disclaimer: This is a PDF file of an unedited manuscript that has been accepted for publication. As a service to our customers we are providing this early version of the manuscript. The manuscript will undergo copyediting, typesetting, and review of the resulting proof before it is published in its final citable form. Please note that during the production process errors may be discovered which could affect the content, and all legal disclaimers that apply to the journal pertain.

Introduction

In cancer research, cell-based assays are widely used for screening of drug candidates and drug delivery systems. Especially, 2D monolayer culture models have become a standard and regular model for cytotoxicity assays due to their simplicity and suitability for high-throughput techniques. However, monolayer or suspension cell cultures are lack of 3D architecture and extracellular matrix, which are two of the main defining properties of the *in vivo* tumors (Cukierman et al., 2001). Besides *in vivo* tumor models, an effective and easy approach in studying the properties of tumors is to culture cancer cells in 3D spheroids. A spheroid is a collection of cancer cells held together by a variety of cell–cell junctions, surface membrane microprojections and extracellular matrix (Sutherland, 1988, Owen and Shoichet, 2010).

3D cancer cell cultures (cancer cell spheroids) have gained a lot of interest after their first application in cancer research (Sutherland et al., 1971). Cancer cell spheroids have found to better reflect the cancer tissue complexity, pathophysiology and microenvironment, thus they better resemble the *in vivo* tumor tissues with regard to tumor shape, cell morphology, growth kinetics, gene expression and drug response (Hall et al., 2004, Goodman et al., 2008). Their 3D structure consisting of extensive amount of ECMs causes a complex interaction with cell-to-cell and microenvironment (Berrier and Yamada, 2007). They also tend to show similar growth kinetics to *in vivo* tumors (Hamilton, 1998). The outer-region cells of a spheroid are actively proliferating, while inner-region cells are in non-proliferative state. Spheroids also contain arrested cells in all phases of the cell cycle (Sutherland, 1988). These properties are crucial for testing anticancer therapeutics (Freyer and Sutherland, 1980, Venkatasubramanian et al., 2008, Wartenberg et al., 2002). It is also important to mention that relative to 2D cultures, spheroids have become a great tool for studying the penetration of anticancer drugs into tumor tissue because they provide the necessary architecture to perform such studies (Minchinton and Tannock, 2006). This combination of heterogeneous cell populations and penetration-limiting properties can cause central necrosis and regions of hypoxia in large spheroids, thus they demonstrate high similarities with avascular tumor microregions and micrometastases (Sutherland, 1988, Friedrich et al., 2007).

It has been noted that the response of spheroids to cytotoxic drugs varies from that of monolayer cell culture not only because of limited penetration (Kerr et al., 1988) but also due to dissimilarity in gene expression and cell–cell communication (Mehta et al., 2012). The efflux transporter protein associated with multidrug resistance, P-glycoprotein (P-gp), is upregulated in the G0/G1 phase cells located at the core of a spheroid but normal levels are present in the G2/M arrested cells (Wartenberg et al., 2002). A number of metabolic and synthetic genes are also upregulated in spheroids (Chang and Hughes-Fulford, 2009). Angiogenesis factors, such as the vascular endothelial growth factor, are also differently expressed depending on the type of culture (Sonoda et al., 2003). In conclusion, resistance to anticancer drugs, known as multidrug resistance (MDR), is dependent on both biochemical and physical obstructions in spheroids such as overexpressed efflux pumps (i.e. P-gp), upregulated pathways (i.e. NF- κ B and PI3K) and limited penetration of drugs into the spheroid (Jang et al., 2003, Durand, 1990).

Paclitaxel (PCL), one of the most prescribed conventional chemotherapeutic agents, acts as microtubule stabilizer and blocks cancer cells in the G2/M phase, thus preventing them from mitosis (Wang et al., 2000). It is also an apoptosis inducer in cancer cells (Sugimura et al., 2004). One of the main drawbacks of its use is that it is also a substrate of P-gp and treatment with PCL induces the overexpression of the efflux pump in the cancer cells (Jang et al., 2001). NF- κ B is a transcription factor that controls the expression of genes involved in a number of physiological responses including differentiation, inflammation, and apoptosis (Pahl, 1999). It also has a role of upregulation of MDR1 that codes the P-gp (Gupta et al., 2010). The PI3K/Akt pathway is also another over-activated pathway in a wide range of tumor types and therefore its over-activation leads to increased cancer-cell survival, proliferation, and growth and it also promotes NF- κ B activity (Romashkova and Makarov, 1999), all affects the success of the chemotherapy with PCL.

Curcumin (CUR), a polyphenol known as diferuloylmethane, has several functions including anticancer activity (Anand et al., 2008, Anand et al., 2010, Yallapu et al., 2012, Nair et al., 2012). But most importantly, CUR is able to downregulate both the PI3K/Akt and NF- κ B pathways independent of each other, thus it can acts as a mediator of chemoresistance by sensitizing cancer cells to a conventional chemotherapeutic agents (Sreekanth et al., 2011, Bava et al., 2011).

The investigation of doxorubicin-loaded and anti-cancer antibody 2C5-modified micelle effect on resistant cancer cell spheroid model has been accomplished previously in our lab (Perche et al., 2012). We have also shown that transferrin (TF)-modified PEG-PE (1,2-Distearoyl-*sn*-glycero-3-phosphoethanolamine-N-[methoxy (polyethylene glycol)-2000]) micelles co-loaded with PCL and CUR demonstrate an enhanced cancer cell killing in the monolayer culture (Abouzeid et al., in press). In the current study, we wanted to evaluate the effect of the micellar PCL/CUR and TF as the targeting ligand on resistant ovarian cancer spheroids and *in vivo* tumors. We hypothesized that (i) micellar encapsulation and delivery would enhance the spheroid/tumor penetration and toxicity of the drugs, and (ii) adding TF as the targeting and endocytosis enhancing ligand would increase the penetration of the micellar systems into the spheroids/tumors. With this in mind, PEG-PE-based mixed micelle formulations co-loaded with PCL and CUR and containing vitamin E as the solubility enhancer were prepared, and TF was used as the targeting ligand. Following micelle characterization, cytotoxicity of these micelle formulations was investigated on resistant ovarian cancer cell line NCI-ADR-RES spheroids compared to monolayers. Cellular association and penetration abilities and apoptosis enhancing properties of the formulations on spheroids were also evaluated. The antitumor activity of the formulations was also tested in mice bearing PCL-resistant ovarian SK-OV-3TR tumor. For better comparison, we have attempted to produce SK-OV-3TR spheroids, but in agreement with what was reported previously in many publications (Vinci et al., 2012, Loessner et al., 2010, Sodek et al., 2009), we faced inconsistent spheroid formation by SK-OV-3TR cells under various conditions, which let us to use another resistant ovarian cancer cell line (NCI-ADR-RES), which has the properties close enough to those of the SK-OV-3TR cells, i.e. apoptosis initiator death receptor CD95 levels and response to the ligand (Algeciras-Schimmich et al., 2003), for spheroid studies.

Materials and Methods

Materials

1,2-Distearoyl-*sn*-glycero-3-phosphoethanolamine-N-[methoxy (polyethylene glycol)-2000] (PEG₂₀₀₀-PE) was purchased from Cordem Pharma International (Plankstadt, Germany). 1,2-dioleoyl-*sn*-glycero-3-phosphoethanolamine (DOPE) and 1,2-dipalmitoyl-*sn*-glycero-3-phosphoethanolamine-N-(lissamine rhodamine B sulfonyl) (Rhodamine-PE) were from Avanti Polar Lipids (Alabaster, AL, USA). *pNP*-PEG₃₄₀₀-*pNP* was purchased from Laysan Bio (Arab, AL). Curcumin (CUR), vitamin E and human holo-transferrin (TF) were purchased from Sigma (St. Louis, MO, USA). Paclitaxel (PCL) was from LC Laboratories (Woburn, MA). Accumax[®] was from Innovative Cell Technologies, Inc. (San Diego, CA). The CellTiter-Glo[®] luminescent cell viability assay kit was from Promega (Fitchburg, WI). All other reagents were of analytical grade.

Cell culture and spheroid formation

Human MDR ovarian cancer NCI-ADR-RES cells (National Cancer Institute, Frederick, MD, USA) were grown at 37°C at 5% CO₂ in DMEM supplemented with 50 U/mL penicillin, 50 (µg/mL streptomycin and 10% FBS (v/v). Multicellular NCI-ADR-RES cancer cell spheroids prepared by liquid overlay method (Perche et al., 2012). Briefly, serum free DMEM medium with 1.5% (w/v) agar was prepared and sterilized. 50 µL of the agar solution were added to the bottom of each well of the 96 well plates to prevent cell adhesion onto the well surface. Plates were allowed to cool down for 45 minutes before use. NCI-ADR-RES cells were trypsinized, counted and then seeded at the density of 12,000 cells/well. Plates were centrifuged for 15 min at 1,500 rcf at 24°C. Spheroid formation was continuously followed using Nikon Eclipse E400 microscope (Nikon Inc., Melville, NY) with the Spot camera and Spot Advanced[™] software (Spot Imaging, Sterling Heights, MI). When the spheroids are formed and dense (after 3–5 days), they were treated with the formulations for various purposes.

SK-OV-3TR cells, PCL-resistant variant of SK-OV-3 human ovarian adenocarcinoma cell line, were a kind gift from Dr. Duan Zhenfeng (MGH, Boston, MA). To produce SK-OV-3TR spheroids, hanging drop method were also tried in addition to liquid overlay method with modifications.

Micelle preparation

PCL and/or CUR drug-loaded mixed micelles were prepared by the thin film hydration method. PCL (1 mg/ml in 0.1% acetic acid-methanol solution) and/or CUR (2 mg/ml in 0.1% acetic acid-methanol solution) at various weight % of the polymer were added to PEG₂₀₀₀-PE and vitamin E (89:11 molar ratio) solution in chloroform. The organic solvents were removed by the rotary evaporation and a thin film of drug/micelle-forming material mixture was formed. This film was further dried overnight in freeze-dryer to remove any residuals of organic solvents (Freezone 4.5 Freeze Dry System, Labconco, Kansas City, MO). Drug-loaded mixed micelles were formed by resuspending the film in phosphate buffered saline (PBS) pH 7.4, to give the final concentration of micelle forming materials of 5 mM in all formulations. Excess non-incorporated drugs were separated by filtration

through a 0.2 μm syringe filter before characterization. Micelle size was measured by the photon correlation spectroscopy (PCS) using a N4 Plus Submicron Particle System (Coulter Corporation, Miami, FL, USA). Zeta potential values of the micelles were determined by using Zeta Plus Particle Analyzer (Brookhaven Instruments Corp, Santa Barbara, CA). Critical micelle concentration (CMC) of the micelles was estimated by standard Pyrene method (Zhao et al., 1990) as described in (Sawant et al., 2008).

Preparation of targeted micelles

To obtain targeted micelles, TF was reacted with *pNP*-PEG₃₄₀₀-PE (Torchilin et al., 2001). Briefly, required amount of *pNP*-PEG₃₄₀₀-PE in chloroform was added into the round bottom flask and polymer film was formed after removing the solvent by rotary evaporation followed by overnight drying under vacuum. The film was hydrated and vortexed first with citrate-buffered saline (CBS) pH 5.0 to prevent early hydrolysis of *pNP* distal groups. After forming micelles, TF solution in PBS (pH 7.4) was added to the mixture, and the pH was adjusted to 8.5 with NaOH. Molar ratio of *pNP* groups to TF was kept at 2:1. Reaction time was overnight at room temperature to allow sufficient TF conjugation and the complete hydrolysis of the unreacted *pNP* groups at the higher pH. TF-micelles were then dialyzed using a 100,000 MWCO cellulose ester membrane against PBS (pH 7.4) for 4 hours to insure the complete removal of the unconjugated TF. TF conjugated micelles were mixed and co-incubated with drug loaded PEG-PE micelles at 1% mole ratio of *pNP*-PEG₃₄₀₀-PE to PEG2000-PE for 4 hours at room temperature. Conjugation efficiency of TF was measured using a micro BCA kit (Pierce, Rockford, IL) according to the manufacturer's instructions. Protein content was determined by comparing TF-modified micelles to a known concentration of TF standards. Absorbances from TF-modified micelle samples were normalized with empty non-targeted micelle samples at the same lipid concentration.

Drug solubilization efficiency of the micelles

Drug incorporation efficiency was measured by a validated RP-HPLC method using a Hitachi Elite LaChrome HPLC system equipped with an autosampler (Pleasanton, CA) and diode array detector. Xbridge C18 (4.6 mm x 250 mm) reverse phase column (Waters Corporation, Milford, MA) was eluted with 60:40 (v/v) acetonitrile:water mobile phase at flow rate of 1 ml/min. PCL was detected at a wavelength of 227 nm, while CUR was detected at 420 nm. Sample injection volume was kept constant at 50 μl and the sample run time was 8 min. The concentration of the drug was determined by measuring the area under curve of the corresponding peaks. Standard curves obtained using the known amounts of drugs in mobile phase, were used to determine the concentration of the incorporated drug in micelles. Drug-loaded micelles were filtered to remove non-incorporated drugs and diluted in the mobile phase to disrupt the micelle structure and release the incorporated drugs for detection. All samples were analyzed in triplicate. Validation parameters were specificity, linearity, precision (repeatability, intermediate precision and reproducibility), accuracy and stability.

Association of micelles with cancer cell spheroids compared to monolayers

Cellular association of TF-targeted or non-targeted micelles was assessed by flow cytometry after 4 hours incubation with resistant ovarian cancer cell monolayers. Briefly, NCI-ADR-RES cells were seeded in 12-well plates at a density of 80,000 cells/well and grown for 24 hours. Then cells were treated with rhodamine-labeled (1% mol) micelle formulations at 1 mg/mL lipid concentration in serum complete media (10% FBS). Same formulations and lipid concentrations were used for investigating the cellular association patterns with spheroids after 1, 4 and 6 hours of incubation time. For monolayers, after the incubation time cells were trypsinized and detached from the wells. Cell suspensions were analyzed with FACSCalibur flow cytometer (Beckton Dickinson, Franklin Lakes, NJ) using 488 nm blue laser for excitation and FL2 channel (585/42 nm) for recording. Cells were gated using forward versus side scatter to gate 10,000 events after excluding debris and dead cells.

Micelle association in spheroids was investigated after incubation of 5-day-old spheroids with rhodamine-labeled micelles. At the determined incubation times, 5 spheroids as one replicate were collected into the tubes to achieve necessary cell number. The spheroids were washed two times with PBS. Following removal of the remaining PBS, AccuMax[®] cell detachment solution was added and tubes were incubated for 10 minutes at 37°C on the horizontal shaker with occasional pipetting. After dispersing of the spheroids into single cells, FBS was added into the tubes to inhibit the AccuMax[®] activity. Cells were centrifuged and dispersed in ice-cold PBS, then immediately analyzed with flow cytometer using the same settings described above. All flow cytometry experiments with monolayers and spheroids were triplicate.

Distribution of micelles in spheroids

Distribution of rhodamine throughout the spheroids was analyzed after 1, 4 and 6 hours incubation of 5-day-old spheroids with rhodamine-labeled non-targeted and TF-targeted micelles in the complete media by a Zeiss LSM 700 confocal microscope. Spheroids were harvested and fixed in 4% paraformaldehyde, then placed in 16-well glass chamber slides (Nunc[™] Lab-Tek[™] Chamber Slide System, USA). Z-stack images of spheroids starting at the apex of each spheroid were collected with 10 µm intervals using 555 nm laser at 1.2%. All images were taken using a 10× objective. Images were analyzed using Image-J software with Fiji package (NIH, Bethesda, MD, version 1.49b). Maximum intensity Z-projection images were also taken to indicate the rhodamine intensity differences in the groups. To evaluate the penetration profiles, rhodamine intensity in the center of the each Z-stack were calculated using corrected integrated pixel density and plotted against the depth.

Transferrin receptor expression in spheroids

Transferrin receptor (TfR) levels in monolayers and spheroids were compared using flow cytometry. NCI-ADR-RES cells were seeded as monolayers in 6-well plates at a density of 4×10⁴ per well. After 24 hours, the cells were washed three times with ice-cold PBS, detached by mechanical scrapping and resuspended in 0.5% bovine serum albumin in PBS. The cell suspensions were incubated either with fluorescein isothiocyanate-labeled (FITC) anti-transferrin receptor monoclonal antibody (Clone B-G24, Abcam, MA, USA) or FITC-labeled isotype control at +4°C at the ratio recommended by the manufacturer. After 30

minutes of incubation, the cells were washed with 0.5% bovine serum albumin in PBS and analyzed by flow cytometry. 488 nm blue laser was used for excitation and FL1 channel was used for recording of 10,000 events. To investigate the TfR levels in spheroids, NCI-ADR-RES spheroids were grown, and at different days were harvested and dissociated with same method as above using AccuMax[®] cell detachment solution. Additionally, spheroids were incubated with the TfR antibody prior to dissociation for 1 hour and then analyzed by flow cytometry. After the single cells were obtained from spheroids, same procedures were done as with monolayers.

cellular viability in spheroids compared to monolayers

The *in vitro* cytotoxicity of the different micellar formulations was investigated against NCI-ADR-RES spheroids compared to monolayers. For monolayer cell viability, Cell Titer Blue[®] (Promega, Madison, WI) viability assay was used according to the manufacturer's protocol. Briefly, cells were seeded into the 96-well plates at a density of 3000 cells/well and grown for 24 hours before treatment. After incubation with the formulations in serum complete media for 72 hours, wells were washed twice and Cell Titer Blue[®] reagent was added into the wells according to the manufacturer's protocol. Obtained cellular viability values were graphed against PBS treated cells as controls.

Cellular viability of the spheroids was determined after 72 hours treatment of 3-day-old spheroids. After the treatment with different formulations, drug concentrations and combinations, all the media from the corresponding wells along with the spheroids were collected and placed in a centrifuge tube. Five spheroids were collected as one replicate to increase the sensitivity. To disperse the spheroids into single cells, same method described with AccuMax[®] cell detachment solution was used. Obtained cells were centrifuged and supernatants were discarded. Complete DMEM and CellTiter-Glo[®] reagent at 1:1 volume ratio was added into the tubes and cells were incubated for 20 minutes for complete cell lysis. Luminescence was measured using multiplate reader by transferring 100 μ L of the solution into 96 well black-walled plates. Cytotoxicity data in the figure are presented as the mean \pm standard deviation. PBS-treated cells were taken as controls to calculate % cell viability, and the treatment was carried out in triplicate and at least 3 different assays.

Detection of phosphatidylserine externalization

Phosphatidylserine (PS) externalization from inner membrane to outer membrane as an indicator of apoptosis was investigated by flow cytometry using annexin V and propidium iodide (PI) (Vermes et al., 1995). NCI-ADR-RES monolayers and 5-day-old spheroids were treated with 5 μ M CUR and/or 0.80 μ M PCL for 72 hours. Briefly, cells were collected from monolayers or spheroids as single cells and washed twice with PBS, resuspended in annexin binding buffer and analyzed using Alexa Fluor[®] 488 annexin V/Dead Cell Apoptosis Kit with Alexa Fluor 488 annexin V and PI (Molecular Probes, Eugene, OR, USA) according to the manufacturer's protocol.

Tumor inhibition studies

Possible correlation between the spheroid model and *in vivo* model of resistant ovarian cancer was investigated on tumors of SK-OV-3TR cells. TF-modified and non-modified

micelles containing CUR and/or PCL were used to investigate the tumor inhibition efficacy of formulations. 6–8 weeks old nude mice were used in the experiments. Weights of the mice were monitored throughout the study as an indicator for toxicity and intolerability of the formulations. When the SK-OV-3TR cells reached to 70% confluency, they were trypsinized and harvested. Cells were then counted and 3 million cells were re-suspended in 200 μL of Matrigel:PBS solution (1:1, v/v). The cell suspensions were injected subcutaneously over the right flank of the animal. Tumors were allowed to grow for approximately 14 days post tumor inoculation and tumor volume was measured regularly. Mice were randomly split into 4 different groups upon tumor reaching 200 mm^3 . All formulations were administered intraperitoneally due to the high injection volume ($\sim 500\mu\text{L}$) at a dose of 25 mg/kg CUR and 10 mg/kg PCL every 3 days. The dose ratio of CUR:PCL was 2.5:1 w/w as determined by in vitro assays. Mice were monitored for changes in their body weight and tumor volumes measured daily with the same Vernier caliper. The measurements were taken in two perpendicular dimensions and tumor volumes were calculated by applying the formula $(L \times W) \times 1/2$, where L is the longest dimension and W is the dimension perpendicular to L. All animals were sacrificed when the control group tumor volumes reached 1000 mm^3 . Tumors from the mice were also collected and weights were recorded.

Results and Discussion

Characterization of co-loaded micelles

All the TF-targeted or non-targeted micelle formulations have the hydrodynamic diameter ranging from 15–20 nm. Zeta potential values of the targeted and non-targeted micelles were -18.9 ± 0.9 mV and -27.7 ± 1.7 mV, respectively. Attachment of TF targeting moiety did not change the micelle size significantly, as reported previously (Sawant et al., 2013). Also, encapsulation of PCL and CUR alone or together did not cause significant differences in the micelle size. CUR and PCL were effectively co-encapsulated into the both TF-targeted and non-targeted micelles at concentrations of 1216.7 ± 82.3 ($\mu\text{g}/\text{mL}$ (3.3 ± 0.2 mM) and 482.5 ± 37.3 ($\mu\text{g}/\text{mL}$ (0.56 ± 0.04 mM), respectively. The weight ratio between the co-loaded CUR and PCL was approximately 2.5:1. There was no significant difference between the encapsulated drug amounts in the micelles when the individual drugs were used. Moreover, TF-modification did not affect the solubilized drug amounts in the micelle formulations. Both CUR and PCL are water insoluble drugs thus, to achieve higher co-loading values vitamin E was added to the formulations. It has been reported that vitamin E acts as a solubility enhancer for the hydrophobic drugs by increasing the hydrophobicity and the volume of the micelle core, resulting in the higher encapsulation values of the non-soluble drugs (Dabholkar et al., 2006, Sawant et al., 2008, Torchilin, 2005).

The TF conjugation efficiency to the micelles was determined by micro BCA assay using TF instead of BSA as the protein standard after the dialysis of TF-PEG₃₄₀₀-PE micelles. The amount of actual TF in the final formulations was calculated as 0.64 mol% of the total lipids, which corresponds to TF concentration of 32 μM . The CMC value for PEG-PE/vitamin E micelles was 1.66×10^{-5} M, in correspondence with the previously reported CMC

values for mixed PEG-PE micelles (Lukyanov and Torchilin, 2004, Mu et al., 2005, Musacchio et al., 2009).

Spheroid Formation

For cancer cells, to build up spheroids, the main requirement is to create forces to prevent cell adhesion to the container wall and thus, generate an environment, which helps the cells to adhere themselves. Several spheroid production methods have been described in literature as spinner flasks (Song et al., 2004, Nyberg et al., 2005), hanging drops (Kelm et al., 2003), matrix culture (Lee et al., 2007), low attachment plates (Vinci et al., 2012), scaffold-based culture (Fischbach et al., 2007) and rotary cell culture (Khaoustov et al., 1999). However, every mentioned technique has limitations such as requirement of specialized equipment, variation in cell number and spheroid size, high shear forces, intensive labor and most importantly difficulties in scale-up and massive production processes. Liquid overlay technique which involves creation of non-adhesive surfaces in cell culture plates and petri dishes by coating of poly-HEMA (hydroxyethyl methacrylate) (Ivascu and Kubbies, 2006, Hoevel et al., 2004) or agar (Friedrich et al., 2009) have been regularly used to produce cancer cell spheroids. The liquid overlay technique with agar coated 96 well plates is proven to give unified, reproducible and dense tumor cell spheroids when compared to the other previously mentioned methods but the main advantages were obtaining single spheroid/well for easy handling and massive spheroid production numbers for high-throughput screening tests. In our study, the spheroid production yield was $94.8 \pm 2.3\%$ with intra-plate coefficient of variation of 2.45%.

According to the classification that has been established by Ivascu and Kubbies (Ivascu and Kubbies, 2007) the resulted spheroids can be classified as tight spheroids with sharp edges and dense structures. The resulted NCI-ADR-RES spheroids have diameters of 1259.0 ± 70.8 , 729.0 ± 46.8 , 523.0 ± 20.4 , 550.3 ± 21.0 and 544.3 ± 23.5 μm at day 0, 1, 3, 5 and 7, respectively. Even though spheroid sizes larger than 500 μm can indicate a central secondary necrosis and hypoxic regions (Kunz-Schughart, 1999), Mikhail et al. demonstrated that those properties can also be cell type dependent, while hypoxic and necrotic core structure could be seen for HT29 but not for HeLa spheroids (Mikhail et al., 2013).

With the SK-OV-3TR cells, however, spheroids with dense structure and sharp edges could not be prepared. The resulting spheroids were loose aggregates as reported in different studies (Ivascu and Kubbies, 2007, Vinci et al., 2012). SK-OV-3TR cells formed aggregates rather than spheroids with liquid overlay and hanging drop methods as reported previously (Sodek et al., 2009) and they were not suitable for handling as the aggregate structure was easily disturbed with pipetting or even adding media into the wells. Recently Loessner *et al.* (Loessner et al., 2010) and Vinci *et al.* (Vinci et al., 2012) reported that with hanging drop or liquid overlay method, SK-OV-3 cells can be formed into spheroids with the addition of synthetic hydrogels or Matrigel™ displaying key features of ECM. However, in our study we decided not to use this kind of hydrogel based materials to minimize the possibility of interference with the cytotoxicity and visualization studies, eliminate the additional steps that have crucial effect on spheroid structure. Thus, we used liquid overlay method for the

reasons that provided above to prepare NCI-ADR-RES ovarian cancer cell spheroids for in vitro studies and SK-OV-3TR ovarian cancer cells for in vivo tumor inhibition studies.

Cellular association and accumulation of the micelles in spheroids

TF is responsible for iron transport into the cells via its receptor (TfR), a receptor overexpressed in many cancer cells than normal cells (Daniels et al., 2012). Targeting the TfR with nano-sized carriers has been shown to increase the endocytosis of the carriers and thus, enhance the intracellular payload delivery (Choi et al., 2010, Sahoo et al., 2004, Shah et al., 2009). Total micelle association with cells includes the fluorescently labeled micelle fraction attached to the surface receptors and the fraction internalized. Figure 1 represents the mean rhodamine fluorescence intensity increase obtained by flow cytometry after the treatment of monolayers and spheroids with rhodamine-labeled micelles. Empty micelles (non-rhodamine containing micelles) showed no rhodamine intensity increase comparing to control cells, indicating that there is no autofluorescence interference from the micelle materials. 4 hours after the treatment of monolayers, the rhodamine intensity increase was $67.67 \pm 3.51\%$ and $74.05 \pm 6.10\%$ respectively for non-targeted and targeted micelles. There was no significant difference related to the targeting, which suggests that in monolayers 4 hours of incubation time is enough for non-modified micelles to associate with the cells in same level as TF-targeted ones.

In spheroids, the intensity was increased significantly with longer incubation times ($P < 0.05$). The intensity increase after 4 hours was less than half of that with monolayers, and even after 6 hours the increase was still significantly lower comparing the monolayers, which indicates the limited penetration of the formulations into the spheroid structure thus less cellular association and internalization of the micelles.

Most of the cancer research involving the drug resistance mainly focuses on the biochemical mechanisms, while the physical limitations of drug penetration and association into the tumor tissues in vivo also plays an underestimated but crucial role (Minchinton and Tannock, 2006). While water-soluble drugs can easily penetrate and distribute into the ECM and tumor tissues, this ability is limited for water insoluble drugs. At the same time, cells that formed spheroids are in close contact with each other and this cell contact can also lead changes in the receptor, protein and gene expression levels of the cells (Oloumi et al., 2002). This alteration in the already P-gp overexpressing resistant cells like NCI-ADR-RES could easily cause limited association and penetration of water-insoluble drugs into the spheroids because of the efflux pump activity and physical barriers in the spheroids.

The only significant difference related to the TF targeting seen after 6 hours of incubation ($P < 0.05$), indicates that cellular association patterns are completely different than monolayers. In a recent report, Perche et al. (Perche et al., 2012) showed that micellar encapsulation of doxorubicin could overcome the limited drug uptake in spheroids. Moreover, further modification of these PEG-PE-based micellar nanocarriers by monoclonal anti-nucleohistone autoantibody 2C5 caused deeper penetration of doxorubicin into the spheroids. In our study, the similar results we obtained suggest that, penetration of the micelles into the spheroids can be further increased using the TF as the targeting moiety.

Choi *et al.* (Choi et al., 2010) indicate that in addition to the TF modification (targeted vs. non-targeted), TF content of the nanocarriers also plays an important role in terms of optimized cellular interaction. In a recent study, Sawant *et al.* used TF as one of the targeting ligands of the dual targeted system and they underlined the importance of the TF content for optimal ligand density. Our TF content of 0.64 mole % in the formulations is in agreement with their reported results and suggests that TF can be successfully used as a targeting and endocytosis enhancing ligand for better spheroid penetration (Sawant et al., 2013).

Accumulation of labeled micelles in spheroids

In order to visualize whether the TF-targeted micelles will have better association and penetration into the spheroids, we analyzed distribution of Rh-labeled micelles, non-targeted and targeted with TF, throughout the spheroids by confocal microscopy (Figure 2). This evaluation has been reported before as the indirect identifier of nanocarrier penetration into the spheroids (Kim et al., 2010, Perche et al., 2012, Wartenberg et al., 1998, Ackerman et al., 2008). The results suggest that, the small size of the micelles allows for the easy penetration into the spheroids as seen in Figure 2A. Both the non-targeted and TF-targeted micelles can be visualized in the layers of the spheroids as can be seen from the Z-stack images. The brightness and contrast settings were kept constant for each image. To evaluate the penetration differences between the formulations and incubation times, maximum pixel intensity (MPI) Z-projections of the stacks were created using Fiji software. MPI creates an output image using the maximum value of each pixel over all images in the stack at the particular pixel location. The corrected pixel densities in the core area of the spheroid sections from Figure 2A were quantified using Fiji software and plotted against the section distance from the apex of the corresponding spheroid. The analysis was carried out through 140 μm depth, however after 100 μm into the spheroid structure, the pixel densities in the core area become very low due to the faltered laser penetration after ~ 70 μm (Verveer et al., 2007, Pampaloni et al., 2007, Carver et al., 2014). It can be seen that the profiles of TF-targeted micelles after 4 and 6 hours of incubation were very similar, indicating the saturation of the penetration with TF targeting. Non-targeted micelles after 6 hours of incubation gave similar pixel intensity profile with the targeted micelles all the way through 30 μm , but their penetration reached the maximum level at 40 μm depth into spheroids, while TF-targeted micelles could reach significantly deeper levels. At 50 μm depth, the pixel densities from the core of the spheroids were quantified and plotted (Figure 2C). This depth was chosen to make a quantitative comparison since at deeper layers, the lack of laser penetration could bring upon misleading data. For every time point, TF-targeted micelles showed significantly higher rhodamine density compared to non-targeted formulations.

While the flow cytometry analysis did not show significant increase in the fluorescence intensity related to the TF modification until 6 hours of incubation of formulations with spheroids, the confocal imaging results suggest a better penetration into the spheroid structure of TF-modified micelles for every time point. This difference can be explained by the difference between the time needed to penetrate into the spheroid structure and the time needed for cellular association. TF-modified micelles could penetrate inside the spheroid better than the non-modified ones, but the significantly higher cellular association and

internalization occurs only after 2 additional hours. We hypothesize that penetration of micelles inside the spheroid occurs through the ECM spacing and tight junctions as well as due to intracellular passage.

The results obtained by flow cytometry (Figure 1) and confocal imaging (Figures 2) supports each other and suggests that PEG-PE based micellar nanocarriers are able to penetrate into the spheroid structure with the benefit of their small size, in agreement with previous studies (Perche et al., 2012, Kim et al., 2010, Han et al., 2009). Moreover, TF-targeting significantly enhances the micelle penetration into the deeper layers of the spheroids.

Transferrin receptor expression in spheroids

Flow cytometry data showing the TfR levels in monolayers and spheroids are given in Figure 3. Three, 5 and 8-day-old spheroids were used to better compare the TfR levels in matured spheroids. The FITC-labeled isotype-matched antibody was used as the baseline control and the mean fluorescence increase associated with TfR-bound antibody was calculated. When the spheroids were pre-treated with labeled antibody, the mean fluorescence increase was very low comparing to the isotype control, which can be explained by 'binding site barrier' hypothesis introduced by Weinstein et al (Juweid et al., 1992), the concept proposing that macromolecular ligands, such as antibodies, could be prevented from penetrating tumors as a consequence of their successful binding to the target receptors on tumor periphery.

As can be seen from the Figure 3, the fluorescence increase in the monolayers compared to isotype control was $71.8 \pm 3.1\%$ higher than that in the spheroids at different days. The TfR expression levels in spheroids compared to monolayer was not significantly lower, although the trend is easily recognizable. TfR is overexpressed in the cancer cells due to the greater iron demand because of fast growth and division. (Daniels et al., 2012, Gomme et al., 2005). The cells in the outer layers of the spheroids are actively dividing, while the cells formed the core of the spheroids enter their quiescent phase, which explains the lowering of TfR levels with increased spheroid maturity. The mean fluorescence increase for 3,5 and 8-day-old spheroids was $68.2 \pm 4.6\%$, $64.1 \pm 3.8\%$ and $51.7 \pm 13.6\%$, respectively. The differences were not significantly lower than monolayers or each other (unpaired samples, t test, $P > 0.05$) except the pre-treated spheroids thus, we believe the effect related to TfR levels was not a primary factor in the cellular association and penetration of the formulations into spheroids but still has to be considered for other ligands or systems.

Cytotoxicity in Monolayers

In vitro ability of micelle formulations to deliver PCL and CUR into the cells was assessed in NCI-ADR-RES monolayers. The response of the cells to PCL or CUR as single agents is shown in Figure 4. Both free drugs, PCL and CUR, showed significantly less cytotoxicity than micellar formulations, and the cell viability response to modified or non-modified micelles were almost the same at all concentrations that were used. Similar to the cellular association results by flow cytometry, the long incubation times with micelle formulations allow them to interact with the cells and be internalized by them, regardless of their

modification with a targeting moiety. On the other hand, clear advantage of micellar encapsulation can also be seen from the figures. IC_{50} values were 2.01, 1.22 and 1.21 μM for PCL solution, non-modified and TF-modified micelles, respectively. Similar response was obtained for CUR with IC_{50} values of 17.37, 10.36 and 10.29 μM for CUR solution, non-modified and TF-modified micelles.

NCI-ADR-RES ovarian cancer cell line is reported to overexpress drug efflux pump P-gp (Dong et al., 2009, Patil et al., 2009, Ludwig et al., 2006) and designated as MDR cell line. Thus, micellar encapsulation, in some extent helps to bypassing the P-gp efflux and delivers the drug inside of the MDR cells, as reported by different authors using different micellar structures (Batrakova and Kabanov, 2008, Kabanov et al., 2002, Zhang et al., 2010, Dabholkar et al., 2006, Li et al., 2010). For PCL and CUR co-delivery as free drugs, 5 and 20 μM CUR concentrations were kept constant and cells were treated as monolayers with various PCL concentrations. For combinations with 5 μM CUR, cell viability values were same as free PCL, since the CUR did not have any cytotoxic effect at that concentration. Combination with 20 μM CUR resulted in insignificant cell viabilities at every PCL concentrations since the saturation of the cytotoxic effect, around 24% (data not shown).

Cell viability results for co-delivered micellar drugs were given in Figure 5. Co-loaded micelles with 20 μM CUR, regardless of the PCL concentration and TF modification, caused the same amount of cell death. All viability values at these combination concentrations were below 10%, approximately 15% lower than that of the free drug combinations at the same concentrations. 5 μM CUR micelles (targeted or non-targeted) did not show any cytotoxicity by themselves. While varying the concentration of PCL in the co-loaded micelles and keeping the CUR concentration constant at 5 μM , the combination delivery resulted in significantly higher toxicity compared to PCL micelles alone. The IC_{50} value for non-modified and TF-modified PCL micelles dropped from 1.22 to 0.64 and 1.21 to 0.67 respectively, without significant difference related to TF modification. Approximately 2-fold decrease in the amount of PCL required to achieve a similar cytotoxic outcome was observed for monolayers. Only at 0.80 μM PCL concentration, the combination treatment with both targeted and non-targeted micelles resulted in significantly higher toxicity (synergistic) compared to additive toxicity of individual micelles. At other PCL concentrations the effect was either additive or antagonist (Figure 6). It was explained and exemplified in a review by Dicko et al. that depending on the concentrations or ratios of the combined drugs in nanocarriers, the final *in vitro* or *in vivo* effect could be synergistic, additive or even antagonistic (Dicko et al., 2010, Mayer and Janoff, 2007).

Cytotoxicity in Spheroids

To investigate the cytotoxic effects of anticancer drugs on spheroids, several different endpoint tests as colony formation assays (Watanabe et al., 2007, Mikhail et al., 2013), live/dead cell identification with membrane permeable and impermeable dyes (Shin et al., 2013), LDH release assays (Perche et al., 2012, Ho et al., 2012, Howes et al., 2007) or spheroid size determination assays (Hirschhaeuser et al., 2010, Kim et al., 2010) were established and used in studies. Even though spheroid visualization and diameter measurement is one of the most popular techniques mentioned above, it does not necessarily mean that cell death and

spheroid integrity reflect and correspond the viable cell numbers in the spheroids. In our study, we found that 72 hours after the treatment mean spheroid diameters were between 530 and 411 μm for all groups, without a clear significant difference between the drug loaded formulations within each other, whether they were modified with TF or not. This result led us to evaluate the influence of adding TF as a targeting moiety with respect to cell viability on the CUR and PCL co-loaded micelles (Figure 7) using the CellTiter-Glo[®] Luminescent Cell Viability Assay. This assay quantifies the amount of ATP present as an indicator of metabolically active cells i.e. live cells and is proven to be sensitive, reproducible and robust (Vinci et al., 2012, Lin et al., 2011, Han et al., 2007, Fey and Wrzesinski, 2012).

Figure 7 represents the cell viability data obtained by spheroids treated with different formulations and free drugs. As can be seen from the figure, free CUR did not exert any cytotoxicity on spheroids even at a high dose as 40 μM . It should be noted that, in monolayer experiments, free CUR IC_{50} value was 17.37 μM and CUR concentrations that have no effect on cell viability were below 5 μM , meaning that 8 times higher doses of CUR did still not cause cell death in spheroids. Free PCL by itself at 6.9 μM caused 80.5 \pm 22.0% cell viability in spheroids, while in monolayers significantly lower dose as 0.80 μM caused same viability. When spheroids treated with combination of free drugs at the given concentrations (40 μM CUR and 6.9 μM PCL) spheroid viability was 83.4 \pm 10.0%, which is not significantly different than the PCL cytotoxicity as single agent due to the ineffectiveness of CUR.

In terms of micellar single drug delivery into the spheroids, it was shown that the micellar CUR has no cytotoxic effects on spheroids at 20 and 40 μM doses. Viability values of spheroids treated with micellar PCL were 67.3 \pm 4.9% and 57.2 \pm 1.1% ($P < 0.05$) at 3.45 and 6.9 μM of PCL concentration, respectively. This increase in the cytotoxicity suggests that micellar encapsulation enhance the cellular uptake and penetration into the spheroids over free drugs, in accordance with published studies (Kim et al., 2009, Perche and Torchilin, 2012, Kim et al., 2010). The high concentrations of the micellar drugs to obtain the mentioned cell death values were significantly higher than the doses used in the monolayer experiments. Even though penetration of drugs into a spheroid is the main rate limiting step for effective drug delivery, altered signaling pathways due to the cell-cell contact and microenvironment such as PI3K/Akt and NF- κ B plays an important role in the resistance to many drugs by the negatively regulating the apoptosis, increasing the cell survival and overexpressing the P-gp. Despite the increase in the cytotoxicity with micellar drug encapsulation and delivery into spheroids comparing the free drugs, the IC_{50} values of both micellar CUR and PCL were still 9.3 and 7.3 times more than monolayer IC_{50} values.

The addition of TF as the targeting ligand did not have any effect of the toxicity of the CUR-loaded micelles. IC_{50} values were 97.18 and 97.02 μM for non-modified and TF-modified CUR micelles, respectively. On the other hand, we did notice that at 3.45 and 6.9 μM of micellar PCL, the viability decreased from 67.3 \pm 4.9% and 57.2 \pm 1.1% for the non-targeted formulation to 41.0 \pm 5.5% and 35.3 \pm 2.7% for the TF-targeted formulation, respectively. At the same time a significant decrease from 8.92 μM to 1.35 μM in the IC_{50} values of micellar PCL was observed with TF targeting. This significant increase in the cytotoxicity shows that

TF-modification of the micelles can further increase their cytotoxicity against spheroids by deeper penetration into the spheroids and at the same time better cellular uptake and accumulation by the individual cells forming spheroids, also in accordance with the previously published data using antibodies as the targeting moiety (Perche et al., 2012). More interestingly, cytotoxicity enhancement over PCL micelles by TF-targeted micelles is 1.64 and 1.62 fold higher at 3.45 and 6.9 μM concentrations, which is almost identical to fluorescence data represented in Figure 3.

With respect to the CUR and PCL co-delivery treatments shown in Figure 7, when CUR was combined with PCL, we did notice a significant decrease in cell viability, from $67.3\pm 4.9\%$ to $51.8\pm 2.7\%$ at 20 μM CUR and 3.45 μM PCL, and from $57.2\pm 1.1\%$ to $43.9\pm 5.9\%$ at 40 μM CUR and 6.9 μM PCL. There are numerous reports showing increased P-gp overexpression and related drug resistance in spheroids compared to monolayers in various cancer cell lines including breast, lung and ovarian ones (Doublie et al., 2012, Kolchinsky and Roninson, 1997, Ponce de Leon and Barrera-Rodriguez, 2005, Walker et al., 2004). It has been shown earlier that co-delivery of anticancer agents with resistance modifiers (Patil et al., 2009, Patel et al., 2011, Wong et al., 2006, Sarisozen et al., 2012a) or therapeutic siRNA molecules (Salzano et al., 2014) in nanocarrier formulations could enhance the cytotoxicity and reverse the MDR on 2D monolayers.

Moreover, TF receptor and thus TF targeted nanocarriers have been shown as an important targeted and effective formulations against various 2D cancer cell lines cultures (Daniels et al., 2012, Daniels et al., 2006), and even have the potential to reverse MDR in P-gp overexpressing cells (Kobayashi et al., 2007). In the current study, in accordance with the previous findings, we found that the addition of TF to the single agent-loaded micelles can also increase their activity. On the other hand, TF modification of the CUR and PCL co-loaded micelles did not have any significant effects on the viability of 3D resistant cancer cell spheroid. Conversely, the difference in the viability values of spheroids treated with TF-targeted PCL micelles, non-targeted co-loaded micelles and TF-targeted co-loaded micelles were not significant ($P>0.05$). This finding suggests that TF-modification is able to enhance the effect of PCL loaded micelles to an extent of co-loading with CUR, while it has no effect on co-loaded micelles. Co-loading of PCL and CUR into the micelles or modifying the only PCL loaded micelles with TF is equally effective in resistant ovarian cancer cell spheroid model. We have showed that PCL and CUR co-loading into the micelles is sufficient enough for optimum cytotoxicity without any need of TF modification.

It has been reported that nanoparticles larger than 100 nm were restricted to the spheroid periphery, while smaller 20 nm and 40 nm nanoparticles could effectively penetrate into the spheroid structure (Goodman et al., 2007, Ng and Pun, 2008). Moreover, collagenase modification of these nanocarriers further increased their penetration properties due to the matrix modulating enzyme activity (Goodman et al., 2007). Our results suggest that micelles with ca.20 nm size and modified with TF as endocytosis enhancer and targeting ligand, allow us to achieve good penetration into the spheroid structure without using any ECM modifier enzymes, as proved with flow cytometry, confocal imaging and cytotoxicity experiments. Moreover, we also demonstrated that co-loading of CUR along with PCL into the micelle structure is also a successful approach to overcome MDR in spheroids, due to

the previously reported (Aggarwal, 1995, Shishodia et al., 2005, Shakibaei et al., 2007) PI3K/Akt and NF- κ B inhibitor effect of CUR.

PS externalization and apoptosis enhancement

We investigated the level of the apoptosis in the spheroids after the treatment in order to evaluate the effect of micellar nanocarrier system and drug co-loading. Staining with annexin V was used as the marker for early apoptosis of the cells with intact cell membrane. The translocation of PS from the inner side of the membrane to the outer surface of the membrane allows annexin V to bind and thus make the apoptotic cells recognizable for flow cytometry experiments via its fluorophore tag. PI was used as the second dye to distinguish the cells with damaged membrane, i.e. necrotic and dead cells. The representative dot plots of the double stained cell populations were given in Figure 8A. In the quadrants, lower left side indicates the normal i.e. non-apoptotic cells. Early apoptotic thus annexin V stained cells and late apoptotic (double stained) cells were in the upper left and upper right side, respectively.

The data given in Figure 8 suggests that treatment with empty and CUR loaded micelles causes apoptosis in some extent. But it should be kept in mind that, 8 days after the seeding early apoptosis became evident due to starting of necrotic core formation. PCL loaded micelles on the other hand caused significantly higher early and late apoptotic cells (Figure 8A). When the spheroids treated with co-loaded micelle formulations, we observed significant increase in the late apoptotic cell ratio (upper right quadrant in Figure 8A) and small but significant decrease in the early apoptotic cells (Figure 8B). These results could suggest that co-loaded micelles resulted more cell death than apoptosis, indicating that addition of CUR accelerate the response to the cytotoxic PCL by regulating the MDR related mechanisms.

Tumor inhibition studies

We have shown that CUR co-loading enhanced the cytotoxicity of PCL on the resistant ovarian cancer spheroids, but the TF-targeting did not result in any further increase in cytotoxicity of co-loaded formulations. To determine whether it is possible to compare the *in vitro* data with *in vivo* and investigate the TF-targeting effect *in vivo*, we have used PCL/CUR co-loaded and TF-targeted PCL/CUR co-loaded micelles. Empty micelles and TF-empty micelles were chosen as control groups for these studies. At the doses chosen, the formulations produced no toxicity *in vivo* as indicated by no significant decrease in body weight throughout the study (data not shown). The main objective of the *in vivo* study was to investigate the TF-targeting effect on the co-loaded micelles and evaluate the possible correlation between the responses of resistant ovarian cancer cell spheroids and live tumors. PEG-PE-based micelles have been shown to easily accumulate in the solid tumors due to the “passive targeting” via the EPR effect, and their ability to stay longer times in the circulation has been reported (Lukyanov et al., 2002, Weissig et al., 1998).

At the end of the *in vivo* study, the tumor volume of the “empty micelle” group reached 1000 mm³ at day 60. As can be seen from the Figure 9A, the tumor growth patterns of the Empty and TF-Empty micelle groups were similar, even though the volumes were slightly

smaller in the TF-modified group. According to the 2-way ANOVA (Bonferroni post-test was applied), tumor volumes between the “empty” and “TF-empty” micelle groups were significantly different only at day 58 and 60 ($P < 0.01$). The combination treatment has exhibited superior tumor growth inhibition, suggesting that combining the anticancer effect of PCL with resistance reversal effect of CUR is a promising approach, even at low PCL dose at 10 mg/kg. On the other hand, TF modification of the co-loaded micelles did not cause significant decrease in the tumor volumes, in accordance with the data obtained from spheroid cytotoxicity experiments. At the end of the *in vivo* studies, the tumors were excised and weighed. The “combination treatment” tumor weights for both TF-modified and non-modified groups were significantly lower compared to control drug-free groups (Figure 9B).

We have found that the results obtained from tumor inhibition and tumor weight studies correlated well with the spheroid toxicity data presented in Figure 7. Even though targeting with TF did not enhance the anticancer activity of the formulations, this translation of data from the 3D *in vitro* assay to the *in vivo* model was an encouraging outcome. Moreover, we demonstrated in both spheroid and *in vivo* resistant ovarian cancer model that, when CUR and PCL co-loaded into the micelles TF modification did not further enhance the cytotoxicity and tumor inhibition over non-targeted micelles. Recently, similar results with PCL and Elacridar co-loaded and 2C5 mAb-targeted micelles have been reported (Sarisozen et al., 2012b). Obtained results shows that we can eliminate the additional steps like conjugation of ligand to the lipid and further dialysis that could cause drug leakage from micelles for preparing TF-targeted micelles, since the same *in vitro* and *in vivo* activity could be achieved when PCL and CUR co-loaded in the micelles.

Conclusion

In the present study, MDR ovarian cancer spheroid model and *in vivo* tumor model were used to evaluate the efficacy of TF-targeted PCL and CUR co-loaded micelles. We have found in spheroid model that significantly higher doses of the drugs need to be used compared the monolayers, to obtain same levels of cytotoxicity due to the altered cellular pathways, overexpression of P-gp and limited penetration due to the 3D structure. TF-targeting provided clear advantages over non-modified micelles in terms of better penetration and cellular association, and significantly increased the cytotoxicity of single agent-loaded micelles. However, when CUR and PCL co-loaded micelles were used, TF-targeting did not further increase the cytotoxicity, both in spheroids and *in vivo* tumors. When CUR and PCL co-loaded micelles were used, further TF-targeting becomes unnecessary for this active compound combination, which eliminates additional steps and improves the overall stability of the micelle system. The effect of co-loading and TF-targeting resulted in similar responses *in vivo* and in the 3D cell culture, which suggests that the spheroid model can be used as an intermediate model for evaluation of co-delivery of anticancer compounds by targeted nanocarriers.

Acknowledgments

This work was supported by the NIH/NCI CCNE grant 5U54CA151881 to Vladimir P. Torchilin. No conflict of interest is declared.

References

- Abouzeid AH, Patel NR, Sarisozen C, Torchilin VP. Transferrin-Targeted Polymeric Micelles Co-Loaded with Curcumin and Paclitaxel: Efficient Killing of Paclitaxel-Resistant Cancer Cells. *Pharmaceutical Research*. in press.
- Ackerman ME, Pawlowski D, Wittrup KD. Effect of antigen turnover rate and expression level on antibody penetration into tumor spheroids. *Mol Cancer Ther*. 2008; 7:2233–2240. [PubMed: 18645032]
- Aggarwal BB. Activation of Transcription Factor NF-kappaB Is Suppressed by Curcumin (Diferuloylmethane). *Journal of Biological Chemistry*. 1995; 270:24995–25000. [PubMed: 7559628]
- Algeciras-Schimmich A, Pietras EM, Barnhart BC, Legembre P, Vijayan S, Holbeck SL, Peter ME. Two CD95 tumor classes with different sensitivities to antitumor drugs. *Proc Natl Acad Sci U S A*. 2003; 100:11445–11450. [PubMed: 14504390]
- Anand P, Nair HB, Sung B, Kunnumakkara AB, Yadav VR, Tekmal RR, Aggarwal BB. Design of curcumin-loaded PLGA nanoparticles formulation with enhanced cellular uptake, and increased bioactivity in vitro and superior bioavailability in vivo. *Biochem Pharmacol*. 2010; 79:330–338. [PubMed: 19735646]
- Anand P, Sundaram C, Jhurani S, Kunnumakkara AB, Aggarwal BB. Curcumin and cancer: an "old-age" disease with an "age-old" solution. *Cancer Lett*. 2008; 267:133–164. [PubMed: 18462866]
- Batrakova EV, Kabanov AV. Pluronic block copolymers: Evolution of drug delivery concept from inert nanocarriers to biological response modifiers. *Journal of Controlled Release*. 2008; 130:98–106. [PubMed: 18534704]
- Bava SV, Sreekanth CN, Thulasidasan AKT, Anto NP, Cheriyan VT, Puliappadamba VT, Menon SG, Ravichandran SD, Anto RJ. Akt is upstream and MAPKs are downstream of NF-kappa B in paclitaxel-induced survival signaling events, which are down-regulated by curcumin contributing to their synergism. *International Journal of Biochemistry & Cell Biology*. 2011; 43:331–341. [PubMed: 20883815]
- Berrier AL, Yamada KM. Cell-matrix adhesion. *J Cell Physiol*. 2007; 213:565–573. [PubMed: 17680633]
- Carver K, Ming X, Juliano RL. Multicellular tumor spheroids as a model for assessing delivery of oligonucleotides in three dimensions. *Mol Ther Nucleic Acids*. 2014; 3:e153. [PubMed: 24618852]
- Chang TT, Hughes-Fulford M. Monolayer and spheroid culture of human liver hepatocellular carcinoma cell line cells demonstrate distinct global gene expression patterns and functional phenotypes. *Tissue Eng Part A*. 2009; 15:559–567. [PubMed: 18724832]
- Choi CH, Alabi CA, Webster P, Davis ME. Mechanism of active targeting in solid tumors with transferrin-containing gold nanoparticles. *Proc Natl Acad Sci U S A*. 2010; 107:1235–1240. [PubMed: 20080552]
- Cukierman E, Pankov R, Stevens DR, Yamada KM. Taking cell-matrix adhesions to the third dimension. *Science*. 2001; 294:1708–1712. [PubMed: 11721053]
- Dabholkar RD, Sawant RM, Mongayt DA, Devarajan PV, Torchilin VP. Polyethylene glycol-phosphatidylethanolamine conjugate (PEG-PE)-based mixed micelles: some properties, loading with paclitaxel, and modulation of P-glycoprotein-mediated efflux. *International journal of pharmaceuticals*. 2006; 315:148–157. [PubMed: 16616818]
- Daniels TR, Bernabeu E, Rodriguez JA, Patel S, Kozman M, Chiappetta DA, Holler E, Ljubimova JY, Helguera G, Penichet ML. The transferrin receptor and the targeted delivery of therapeutic agents against cancer. *Biochim Biophys Acta*. 2012; 1820:291–317. [PubMed: 21851850]
- Daniels TR, Delgado T, Helguera G, Penichet ML. The transferrin receptor part II: targeted delivery of therapeutic agents into cancer cells. *Clin Immunol*. 2006; 121:159–176. [PubMed: 16920030]
- Dicko A, Mayer LD, Tardi PG. Use of nanoscale delivery systems to maintain synergistic drug ratios in vivo. *Expert Opin Drug Deliv*. 2010; 7:1329–1341. [PubMed: 21118030]

- Dong X, Mattingly CA, Tseng MT, Cho MJ, Liu Y, Adams VR, Mumper RJ. Doxorubicin and paclitaxel-loaded lipid-based nanoparticles overcome multidrug resistance by inhibiting P-glycoprotein and depleting ATP. *Cancer Res.* 2009; 69:3918–3926. [PubMed: 19383919]
- Doublier S, Belisario DC, Polimeni M, Annaratone L, Riganti C, Allia E, Ghigo D, Bosia A, Sapino A. HIF-1 activation induces doxorubicin resistance in MCF7 3-D spheroids via P-glycoprotein expression: a potential model of the chemo-resistance of invasive micropapillary carcinoma of the breast. *BMC Cancer.* 2012; 12:4. [PubMed: 22217342]
- Durand RE. Slow penetration of anthracyclines into spheroids and tumors: a therapeutic advantage? *Cancer Chemother Pharmacol.* 1990; 26:198–204. [PubMed: 2357767]
- Fey SJ, Wrzesinski K. Determination of drug toxicity using 3D spheroids constructed from an immortal human hepatocyte cell line. *Toxicol Sci.* 2012; 127:403–411. [PubMed: 22454432]
- Fischbach C, Chen R, Matsumoto T, Schmelzle T, Brugge JS, Polverini PJ, Mooney DJ. Engineering tumors with 3D scaffolds. *Nat Methods.* 2007; 4:855–860. [PubMed: 17767164]
- Freyer JP, Sutherland RM. Selective dissociation and characterization of cells from different regions of multicell tumor spheroids. *Cancer Res.* 1980; 40:3956–3965. [PubMed: 7471046]
- Friedrich J, Ebner R, Kunz-Schughart LA. Experimental anti-tumor therapy in 3-D: spheroids--old hat or new challenge? *Int J Radiat Biol.* 2007; 83:849–871. [PubMed: 18058370]
- Friedrich J, Seidel C, Ebner R, Kunz-Schughart LA. Spheroid-based drug screen: considerations and practical approach. *Nat Protoc.* 2009; 4:309–324. [PubMed: 19214182]
- Gomme PT, Mccann KB, Bertolini J. Transferrin: structure, function and potential therapeutic actions. *Drug Discov Today.* 2005; 10:267–273. [PubMed: 15708745]
- Goodman TT, Ng CP, Pun SH. 3-D tissue culture systems for the evaluation and optimization of nanoparticle-based drug carriers. *Bioconjug Chem.* 2008; 19:1951–1959. [PubMed: 18788773]
- Goodman TT, Olive PL, Pun SH. Increased nanoparticle penetration in collagenase-treated multicellular spheroids. *Int J Nanomedicine.* 2007; 2:265–274. [PubMed: 17722554]
- Gupta SC, Sundaram C, Reuter S, Aggarwal BB. Inhibiting NF-kappa B activation by small molecules as a therapeutic strategy. *Biochimica Et Biophysica Acta-Genes Regulatory Mechanisms.* 2010; 1799:775–787.
- Hall MD, Martin C, Ferguson DJ, Phillips RM, Hambley TW, Callaghan R. Comparative efficacy of novel platinum(IV) compounds with established chemotherapeutic drugs in solid tumour models. *Biochem Pharmacol.* 2004; 67:17–30. [PubMed: 14667925]
- Hamilton G. Multicellular spheroids as an in vitro tumor model. *Cancer Letters.* 1998; 131:29–34. [PubMed: 9839617]
- Han M, Bae Y, Nishiyama N, Miyata K, Oba M, Kataoka K. Transfection study using multicellular tumor spheroids for screening non-viral polymeric gene vectors with low cytotoxicity and high transfection efficiencies. *J Control Release.* 2007; 121:38–48. [PubMed: 17582637]
- Han M, Oba M, Nishiyama N, Kano MR, Kizaka-Kondoh S, Kataoka K. Enhanced percolation and gene expression in tumor hypoxia by PEGylated polyplex micelles. *Mol Ther.* 2009; 17:1404–1410. [PubMed: 19471245]
- Hirschhaeuser F, Menne H, Dittfeld C, West J, Mueller-Klieser W, Kunz-Schughart LA. Multicellular tumor spheroids: An underestimated tool is catching up again. *Journal of Biotechnology.* 2010; 148:3–15. [PubMed: 20097238]
- Ho WY, Yeap SK, Ho CL, Rahim RA, Alitheen NB. Development of multicellular tumor spheroid (MCTS) culture from breast cancer cell and a high throughput screening method using the MTT assay. *PLoS One.* 2012; 7:e44640. [PubMed: 22970274]
- Hoebel T, Macek R, Swisshelm K, Kubbies M. Reexpression of the TJ protein CLDN1 induces apoptosis in breast tumor spheroids. *Int J Cancer.* 2004; 108:374–383. [PubMed: 14648703]
- Howes AL, Chiang GG, Lang ES, Ho CB, Powis G, Vuori K, Abraham RT. The phosphatidylinositol 3-kinase inhibitor, PX-866, is a potent inhibitor of cancer cell motility and growth in three-dimensional cultures. *Molecular Cancer Therapeutics.* 2007; 6:2505–2514. [PubMed: 17766839]
- Ivascu A, Kubbies M. Rapid generation of single-tumor spheroids for high-throughput cell function and toxicity analysis. *J Biomol Screen.* 2006; 11:922–932. [PubMed: 16973921]
- Ivascu A, Kubbies M. Diversity of cell-mediated adhesions in breast cancer spheroids. *Int J Oncol.* 2007; 31:1403–1413. [PubMed: 17982667]

- Jang SH, Wientjes MG, Au JL. Kinetics of P-glycoprotein-mediated efflux of paclitaxel. *J Pharmacol Exp Ther.* 2001; 298:1236–1242. [PubMed: 11504826]
- Jang SH, Wientjes MG, Lu D, Au JL. Drug delivery and transport to solid tumors. *Pharm Res.* 2003; 20:1337–1350. [PubMed: 14567626]
- Juweid M, Neumann R, Paik C, Perez-Bacete MJ, Sato J, Van Osdol W, Weinstein JN. Micropharmacology of monoclonal antibodies in solid tumors: direct experimental evidence for a binding site barrier. *Cancer Res.* 1992; 52:5144–5153. [PubMed: 1327501]
- Kabanov AV, Batrakova EV, Alakhov VY. Pluronic block copolymers for overcoming drug resistance in cancer. *Adv Drug Deliv Rev.* 2002; 54:759–779. [PubMed: 12204601]
- Kelm JM, Timmins NE, Brown CJ, Fussenegger M, Nielsen LK. Method for generation of homogeneous multicellular tumor spheroids applicable to a wide variety of cell types. *Biotechnol Bioeng.* 2003; 83:173–180. [PubMed: 12768623]
- Kerr DJ, Wheldon TE, Hydns S, Kaye SB. Cytotoxic drug penetration studies in multicellular tumour spheroids. *Xenobiotica.* 1988; 18:641–648. [PubMed: 3166552]
- Khaoustov VI, Darlington GJ, Soriano HE, Krishnan B, Risin D, Pellis NR, Yoffe B. Induction of three-dimensional assembly of human liver cells by simulated microgravity. *In Vitro Cell Dev Biol Anim.* 1999; 35:501–509. [PubMed: 10548431]
- Kim D, Gao ZG, Lee ES, Bae YH. In vivo evaluation of doxorubicin-loaded polymeric micelles targeting folate receptors and early endosomal pH in drug-resistant ovarian cancer. *Mol Pharm.* 2009; 6:1353–1362. [PubMed: 19507896]
- Kim TH, Mount CW, Gombotz WR, Pun SH. The delivery of doxorubicin to 3-D multicellular spheroids and tumors in a murine xenograft model using tumor-penetrating triblock polymeric micelles. *Biomaterials.* 2010; 31:7386–7397. [PubMed: 20598741]
- Kobayashi T, Ishida T, Okada Y, Ise S, Harashima H, Kiwada H. Effect of transferrin receptor-targeted liposomal doxorubicin in P-glycoprotein-mediated drug resistant tumor cells. *Int J Pharm.* 2007; 329:94–102. [PubMed: 16997518]
- Kolchinsky A, Roninson IB. Drug resistance conferred by MDR1 expression in spheroids formed by glioblastoma cell lines. *Anticancer Res.* 1997; 17:3321–3327. [PubMed: 9413166]
- Kunz-Schughart LA. Multicellular tumor spheroids: intermediates between monolayer culture and in vivo tumor. *Cell Biology International.* 1999; 23:157–161. [PubMed: 10562436]
- Lee GY, Kenny PA, Lee EH, Bissell MJ. Three-dimensional culture models of normal and malignant breast epithelial cells. *Nat Methods.* 2007; 4:359–365. [PubMed: 17396127]
- Li XR, Li PZ, Zhang YH, Zhou YX, CHEN Xw, Huang YQ, Liu Y. Novel Mixed Polymeric Micelles for Enhancing Delivery of Anticancer Drug and Overcoming Multidrug Resistance in Tumor Cell Lines Simultaneously. *Pharmaceutical Research.* 2010; 27:1498–1511. [PubMed: 20411408]
- Lin C-C, Raza A, Shih H. PEG hydrogels formed by thiol-ene photo-click chemistry and their effect on the formation and recovery of insulin-secreting cell spheroids. *Biomaterials.* 2011; 32:9685–9695. [PubMed: 21924490]
- Loessner D, Stok KS, Lutolf MP, Huttmacher DW, Clements JA, Rizzi SC. Bioengineered 3D platform to explore cell-ECM interactions and drug resistance of epithelial ovarian cancer cells. *Biomaterials.* 2010; 31:8494–8506. [PubMed: 20709389]
- Ludwig JA, Szakacs G, Martin SE, Chu BF, Cardarelli C, Sauna ZE, Caplen NJ, Fales HM, Ambudkar SV, Weinstein JN, Gottesman MM. Selective toxicity of NSC73306 in MDR1-positive cells as a new strategy to circumvent multidrug resistance in cancer. *Cancer Res.* 2006; 66:4808–4815. [PubMed: 16651436]
- Lukyanov AN, Gao Z, Mazzola L, Torchilin VP. Polyethylene glycol-diacyl lipid micelles demonstrate increased acculumation in subcutaneous tumors in mice. *Pharm Res.* 2002; 19:1424–1429. [PubMed: 12425458]
- Lukyanov AN, Torchilin VP. Micelles from lipid derivatives of water-soluble polymers as delivery systems for poorly soluble drugs. *Adv Drug Deliv Rev.* 2004; 56:1273–1289. [PubMed: 15109769]
- Mayer LD, Janoff AS. Optimizing combination chemotherapy by controlling drug ratios. *Mol Interv.* 2007; 7:216–223. [PubMed: 17827442]

- Mehta G, Hsiao AY, Ingram M, Luker GD, Takayama S. Opportunities and challenges for use of tumor spheroids as models to test drug delivery and efficacy. *Journal of Controlled Release*. 2012; 164:192–204. [PubMed: 22613880]
- Mikhail AS, Eetezadi S, Allen C. Multicellular tumor spheroids for evaluation of cytotoxicity and tumor growth inhibitory effects of nanomedicines in vitro: a comparison of docetaxel-loaded block copolymer micelles and Taxotere(R). *PLoS One*. 2013; 8:e62630. [PubMed: 23626842]
- Minchinton AI, Tannock IF. Drug penetration in solid tumours. *Nat Rev Cancer*. 2006; 6:583–592. [PubMed: 16862189]
- Mu L, Elbayoumi TA, Torchilin VP. Mixed micelles made of poly(ethylene glycol)-phosphatidylethanolamine conjugate and d-alpha-tocopheryl polyethylene glycol 1000 succinate as pharmaceutical nanocarriers for camptothecin. *International journal of pharmaceutics*. 2005; 306:142–149. [PubMed: 16242875]
- Musacchio T, Laquintana V, Latrofa A, Trapani G, Torchilin VP. PEG-PE micelles loaded with paclitaxel and surface-modified by a PBR-ligand: synergistic anticancer effect. *Molecular pharmaceutics*. 2009; 6:468–479. [PubMed: 19718800]
- Nair KL, Thulasidasan AK, Deepa G, Anto RJ, Kumar GS. Purely aqueous PLGA nanoparticulate formulations of curcumin exhibit enhanced anticancer activity with dependence on the combination of the carrier. *Int J Pharm*. 2012; 425:44–52. [PubMed: 22266528]
- Ng CP, Pun SH. A perfusable 3D cell-matrix tissue culture chamber for in situ evaluation of nanoparticle vehicle penetration and transport. *Biotechnol Bioeng*. 2008; 99:1490–1501. [PubMed: 17969174]
- Nyberg SL, Hardin J, Amiot B, Argikar UA, Rimmel RP, Rinaldo P. Rapid, large-scale formation of porcine hepatocyte spheroids in a novel spheroid reservoir bioartificial liver. *Liver Transpl*. 2005; 11:901–910. [PubMed: 16035089]
- Oloumi A, Lam W, Banath JP, Olive PL. Identification of genes differentially expressed in V79 cells grown as multicell spheroids. *Int J Radiat Biol*. 2002; 78:483–492. [PubMed: 12065053]
- Owen SC, Shoichet MS. Design of three-dimensional biomimetic scaffolds. *J Biomed Mater Res A*. 2010; 94:1321–1331. [PubMed: 20597126]
- Pahl HL. Activators and target genes of Rel/NF-kappaB transcription factors. *Oncogene*. 1999; 18:6853–6866. [PubMed: 10602461]
- Pampaloni F, Reynaud EG, Stelzer EH. The third dimension bridges the gap between cell culture and live tissue. *Nat Rev Mol Cell Biol*. 2007; 8:839–845. [PubMed: 17684528]
- Patel NR, Rathi A, Mongayt D, Torchilin VP. Reversal of multidrug resistance by co-delivery of tariquidar (XR9576) and paclitaxel using long-circulating liposomes. *International journal of pharmaceutics*. 2011
- Patil Y, Sadhukha T, Ma L, Panyam J. Nanoparticle-mediated simultaneous and targeted delivery of paclitaxel and tariquidar overcomes tumor drug resistance. *Journal of Controlled Release*. 2009; 136:21–29. [PubMed: 19331851]
- Perche F, Patel NR, Torchilin VP. Accumulation and toxicity of antibody-targeted doxorubicin-loaded PEG-PE micelles in ovarian cancer cell spheroid model. *J Control Release*. 2012; 164:95–102. [PubMed: 22974689]
- Perche F, Torchilin VP. Cancer cell spheroids as a model to evaluate chemotherapy protocols. *Cancer Biology & Therapy*. 2012; 13:1205–1213. [PubMed: 22892843]
- Ponce de leon V, Barrera-Rodriguez R. Changes in P-glycoprotein activity are mediated by the growth of a tumour cell line as multicellular spheroids. *Cancer Cell Int*. 2005; 5:20. [PubMed: 16001980]
- Romashkova JA, Makarov SS. NF-kappa B is a target of AKT in anti-apoptotic PDGF signalling. *Nature*. 1999; 401:86–90. [PubMed: 10485711]
- Sahoo SK, Ma W, Labhasetwar V. Efficacy of transferrin-conjugated paclitaxel-loaded nanoparticles in a murine model of prostate cancer. *Int J Cancer*. 2004; 112:335–340. [PubMed: 15352049]
- Salzano G, Riehle R, Navarro G, Perche F, De Rosa G, Torchilin VP. Polymeric micelles containing reversibly phospholipid-modified anti-survivin siRNA: a promising strategy to overcome drug resistance in cancer. *Cancer Lett*. 2014; 343:224–231. [PubMed: 24099916]

- Sarisozen C, Vural I, Levchenko T, Hincal AA, Torchilin VP. Long-circulating PEG-PE micelles co-loaded with paclitaxel and elacridar (GG918) overcome multidrug resistance. *Drug Deliv.* 2012a; 19:363–370. [PubMed: 23030458]
- Sarisozen C, Vural I, Levchenko T, Hincal AA, Torchilin VP. PEG-PE-based micelles co-loaded with paclitaxel and cyclosporine A or loaded with paclitaxel and targeted by anticancer antibody overcome drug resistance in cancer cells. *Drug Deliv.* 2012b; 19:169–176. [PubMed: 22506922]
- Sawant RR, Jhaveri AM, Koshkaryev A, Qureshi F, Torchilin VP. The effect of dual ligand-targeted micelles on the delivery and efficacy of poorly soluble drug for cancer therapy. *J Drug Target.* 2013; 21:630–638. [PubMed: 23594094]
- Sawant RR, Sawant RM, Torchilin VP. Mixed PEG-PE/vitamin E tumor-targeted immunomicelles as carriers for poorly soluble anti-cancer drugs: improved drug solubilization and enhanced in vitro cytotoxicity. *European journal of pharmaceuticals and biopharmaceutics : official journal of Arbeitsgemeinschaft fur Pharmazeutische Verfahrenstechnik e.V.* 2008; 70:51–57. [PubMed: 18583114]
- Shah N, Chaudhari K, Dantuluri P, Murthy RS, Das S. Paclitaxel-loaded PLGA nanoparticles surface modified with transferrin and Pluronic(R)P85, an in vitro cell line and in vivo biodistribution studies on rat model. *J Drug Target.* 2009; 17:533–542. [PubMed: 19530913]
- Shakibaei M, John T, Schulze-Tanzil G, Lehmann I, Mobasheri A. Suppression of NF-kappaB activation by curcumin leads to inhibition of expression of cyclo-oxygenase-2 and matrix metalloproteinase-9 in human articular chondrocytes: Implications for the treatment of osteoarthritis. *Biochem Pharmacol.* 2007; 73:1434–1445. [PubMed: 17291458]
- Shin CS, Kwak B, Han B, Park K. Development of an in vitro 3D tumor model to study therapeutic efficiency of an anticancer drug. *Mol Pharm.* 2013; 10:2167–2175. [PubMed: 23461341]
- Shishodia S, Amin HM, Lai R, Aggarwal BB. Curcumin (diferuloylmethane) inhibits constitutive NF-kappaB activation, induces G1/S arrest, suppresses proliferation, and induces apoptosis in mantle cell lymphoma. *Biochem Pharmacol.* 2005; 70:700–713. [PubMed: 16023083]
- Sodek KL, Ringuette MJ, Brown TJ. Compact spheroid formation by ovarian cancer cells is associated with contractile behavior and an invasive phenotype. *Int J Cancer.* 2009; 124:2060–2070. [PubMed: 19132753]
- Song H, David O, Clejan S, Giordano CL, Pappas-Lebeau H, Xu L, O'Connor KC. Spatial composition of prostate cancer spheroids in mixed and static cultures. *Tissue Eng.* 2004; 10:1266–1276. [PubMed: 15363181]
- Sonoda T, Kobayashi H, Kaku T, Hirakawa T, Nakano H. Expression of angiogenesis factors in monolayer culture, multicellular spheroid and in vivo transplanted tumor by human ovarian cancer cell lines. *Cancer Lett.* 2003; 196:229–237. [PubMed: 12860281]
- Sreekanth CN, Bava SV, Sreekumar E, Anto RJ. Molecular evidences for the chemosensitizing efficacy of liposomal curcumin in paclitaxel chemotherapy in mouse models of cervical cancer. *Oncogene.* 2011; 30:3139–3152. [PubMed: 21317920]
- Sugimura M, Sagae S, Ishioka S, Nishioka Y, Tsukada K, Kudo R. Mechanisms of paclitaxel-induced apoptosis in an ovarian cancer cell line and its paclitaxel-resistant clone. *Oncology.* 2004; 66:53–61. [PubMed: 15031599]
- Sutherland RM. Cell and environment interactions in tumor microregions: the multicell spheroid model. *Science.* 1988; 240:177–184. [PubMed: 2451290]
- Sutherland RM, McCreddie JA, Inch WR. Growth of multicell spheroids in tissue culture as a model of nodular carcinomas. *J Natl Cancer Inst.* 1971; 46:113–120. [PubMed: 5101993]
- Torchilin VP. Lipid-core micelles for targeted drug delivery. *Curr Drug Deliv.* 2005; 2:319–327. [PubMed: 16305435]
- Torchilin VP, Levchenko TS, Lukyanov AN, Khaw BA, Klibanov AL, Rammohan R, Samokhin GP, Whiteman KR. p-Nitrophenylcarbonyl-PEG-PE-liposomes: fast and simple attachment of specific ligands, including monoclonal antibodies, to distal ends of PEG chains via p-nitrophenylcarbonyl groups. *Biochim Biophys Acta.* 2001; 1511:397–411. [PubMed: 11286983]
- Venkatasubramanian R, Henson MA, Forbes NS. Integrating cell-cycle progression, drug penetration and energy metabolism to identify improved cancer therapeutic strategies. *J Theor Biol.* 2008; 253:98–117. [PubMed: 18402980]

- Vermes I, Haanen C, Steffens-Nakken H, Reutelingsperger C. A novel assay for apoptosis. Flow cytometric detection of phosphatidylserine expression on early apoptotic cells using fluorescein labelled Annexin V. *J Immunol Methods*. 1995; 184:39–51. [PubMed: 7622868]
- Verveer PJ, Swoger J, Pampaloni F, Greger K, Marcello M, Stelzer EH. High-resolution three-dimensional imaging of large specimens with light sheet-based microscopy. *Nat Methods*. 2007; 4:311–313. [PubMed: 17339847]
- Vinci M, Gowan S, Boxall F, Patterson L, Zimmermann M, Court W, Lomas C, Mendiola M, Hardisson D, Eccles SA. Advances in establishment and analysis of three-dimensional tumor spheroid-based functional assays for target validation and drug evaluation. *BMC Biol*. 2012; 10:29. [PubMed: 22439642]
- Walker J, Martin C, Callaghan R. Inhibition of P-glycoprotein function by XR9576 in a solid tumour model can restore anticancer drug efficacy. *Eur J Cancer*. 2004; 40:594–605. [PubMed: 14962729]
- Wang TH, Wang HS, Soong YK. Paclitaxel-induced cell death: where the cell cycle and apoptosis come together. *Cancer*. 2000; 88:2619–2628. [PubMed: 10861441]
- Wartenberg M, Fischer K, Hescheler J, Sauer H. Modulation of intrinsic P-glycoprotein expression in multicellular prostate tumor spheroids by cell cycle inhibitors. *Biochim Biophys Acta*. 2002; 1589:49–62. [PubMed: 11909640]
- Wartenberg M, Hescheler J, Acker H, Diederhagen H, Sauer H. Doxorubicin distribution in multicellular prostate cancer spheroids evaluated by confocal laser scanning microscopy and the "optical probe technique". *Cytometry*. 1998; 31:137–145. [PubMed: 9482283]
- Watanabe N, Hirayama R, Kubota N. The chemopreventive flavonoid apigenin confers radiosensitizing effect in human tumor cells grown as monolayers and spheroids. *J Radiat Res*. 2007; 48:45–50. [PubMed: 17132915]
- Weissig V, Whiteman KR, Torchilin VP. Accumulation of protein-loaded long-circulating micelles and liposomes in subcutaneous Lewis lung carcinoma in mice. *Pharm Res*. 1998; 15:1552–1556. [PubMed: 9794497]
- Wong HL, Bendayan R, Rauth AM, Wu XY. Simultaneous delivery of doxorubicin and GG918 (Elacridar) by new Polymer-Lipid Hybrid Nanoparticles (PLN) for enhanced treatment of multidrug-resistant breast cancer. *Journal of Controlled Release*. 2006; 116:275–284. [PubMed: 17097178]
- Yallapu MM, Dobberpohl MR, Maher DM, Jaggi M, Chauhan SC. Design of curcumin loaded cellulose nanoparticles for prostate cancer. *Curr Drug Metab*. 2012; 13:120–128. [PubMed: 21892919]
- Zhang W, Shi Y, Chen Y, Yu S, Hao J, Luo J, Sha X, Fang X. Enhanced antitumor efficacy by paclitaxel-loaded pluronic P123/F127 mixed micelles against non-small cell lung cancer based on passive tumor targeting and modulation of drug resistance. *European journal of pharmaceutics and biopharmaceutics : official journal of Arbeitsgemeinschaft fur Pharmazeutische Verfahrenstechnik e.V*. 2010; 75:341–353. [PubMed: 20451605]
- Zhao CL, Winnik MA, Riess G, Croucher MD. Fluorescence Probe Techniques Used to Study Micelle Formation in Water-Soluble Block Copolymers. *Langmuir*. 1990; 6:514–516.

Highlights

- Paclitaxel and curcumin co-loading shows synergistic anticancer effect
- TF targeting provides better spheroid penetration over non-targeted micelles
- Co-loading and TF-targeting provide similar responses in vitro and in vivo
- Spheroid model can be used to evaluate the targeted nanocarriers

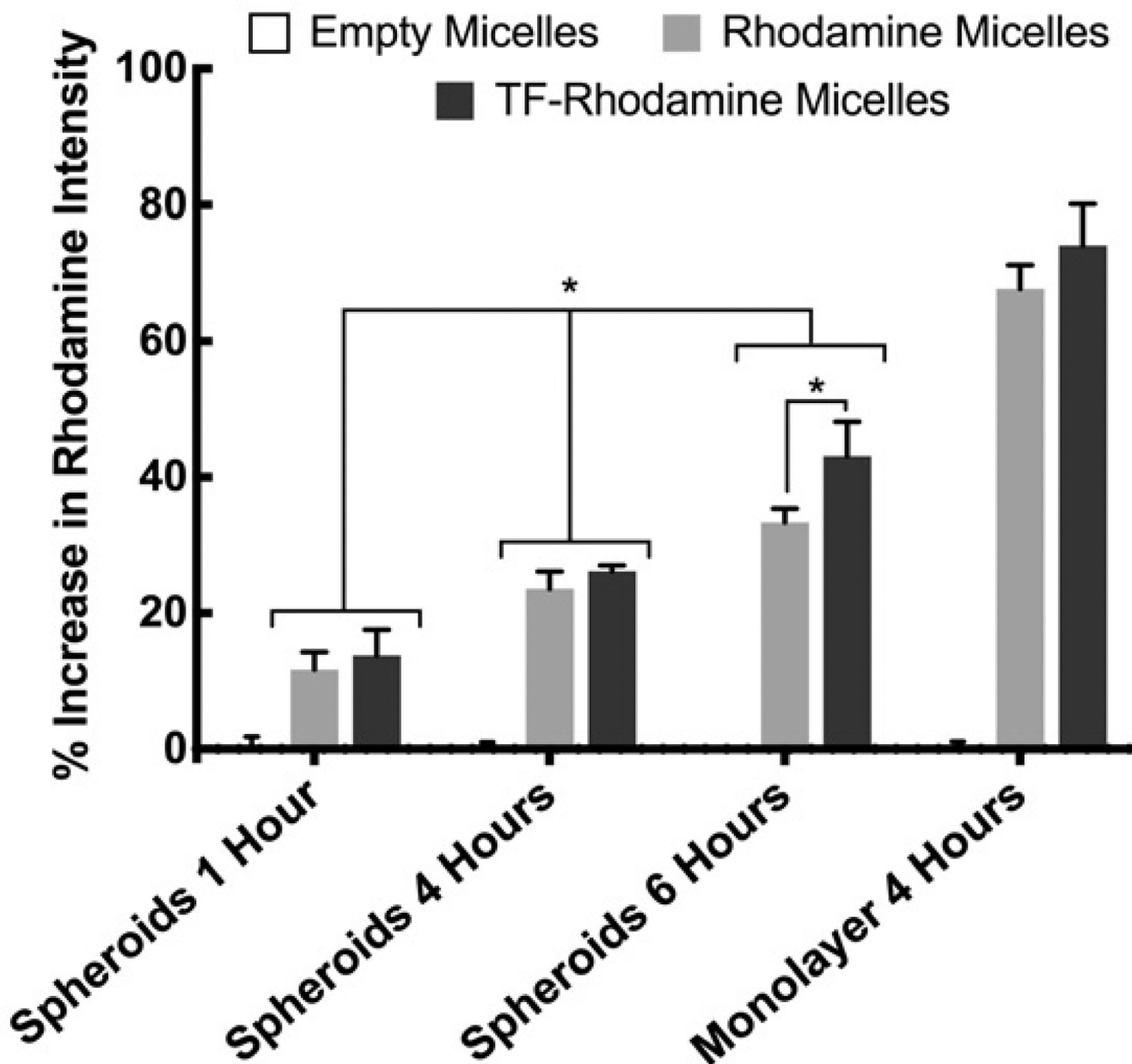


Figure 1.

% Increase in rhodamine intensity after incubation of monolayers and spheroids with rhodamine-labeled formulations for different time points. Results given as mean \pm standard deviation of three independent replications, each $n=3$, * $P<0.05$.

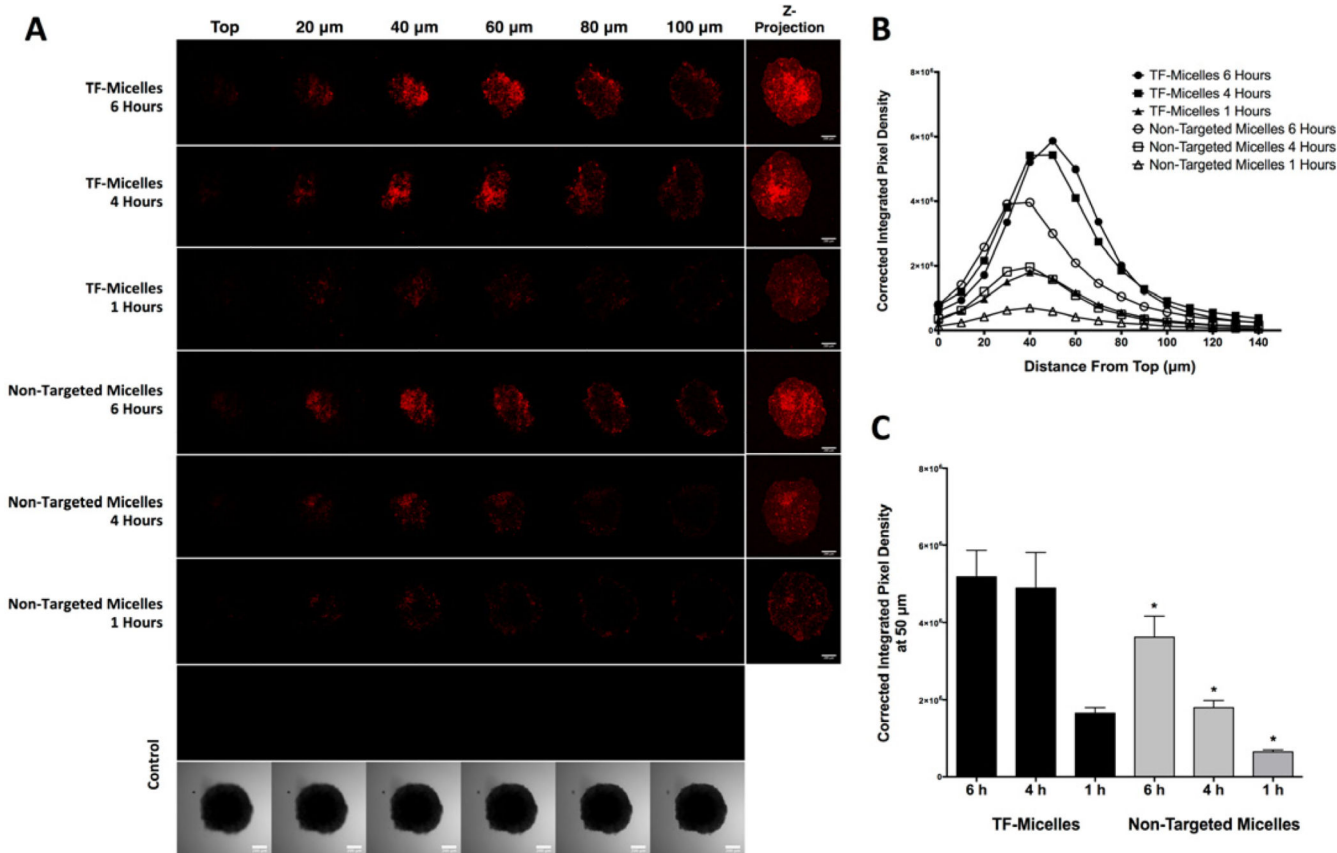


Figure 2. Penetration of TF-targeted and non-targeted micelles throughout NCI-ADR-RES spheroids. NCI-ADR-RES spheroids were incubated for different time points with the formulations. (A) The distribution of micelles was analyzed by confocal microscopy using Z-stack imaging with 10 μm intervals. Scale bars represents 200 μm. Brightness and contrast were modified but kept constant in each image. (B) Corrected integrated pixel density as an indicator of rhodamine intensity was quantified in the core area of each slice of the spheroids from (A). (C) Mean rhodamine intensity at 50 μm depth of the spheroids after the incubation with the formulations. Error bars represents standard deviation, n=3. *P<0.05 using unpaired t test with Welch’s correction.

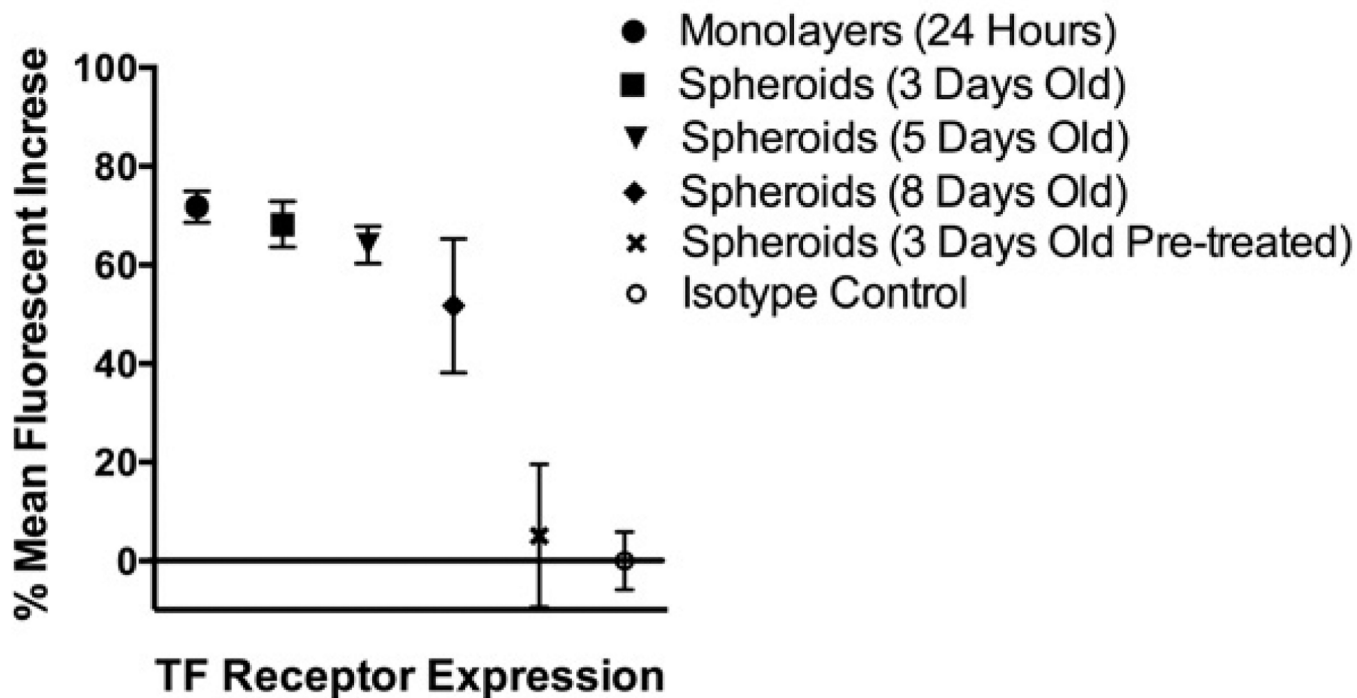


Figure 3.

Flow cytometry analysis of TfR expression in NCI-ADR-RES cell monolayers and spheroids at different days. Isotype-matched FITC-labeled IgG1 monoclonal antibody was used as control. Results indicate the mean intensity increase coming from TfR-bound FITC-labeled anti-Transferrin receptor antibody. Error bars indicate mean±standart deviation, n=3.

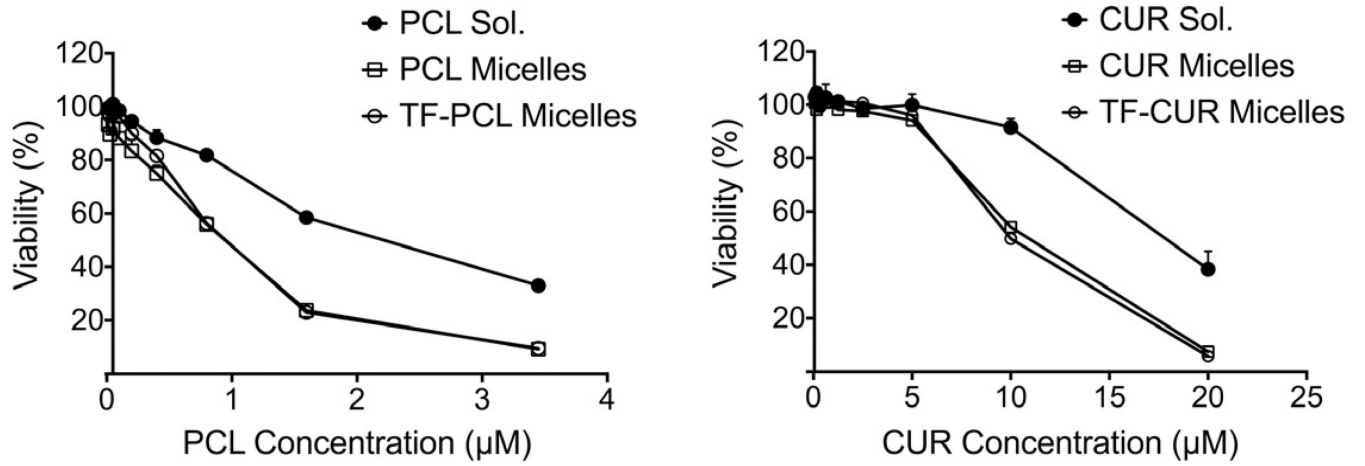


Figure 4. Cell viability of NCI-ADR-RES cells after 72 hours of continuous incubation with single free and micellar drugs at various concentrations. Error bars indicate mean±standart deviation, n=5.

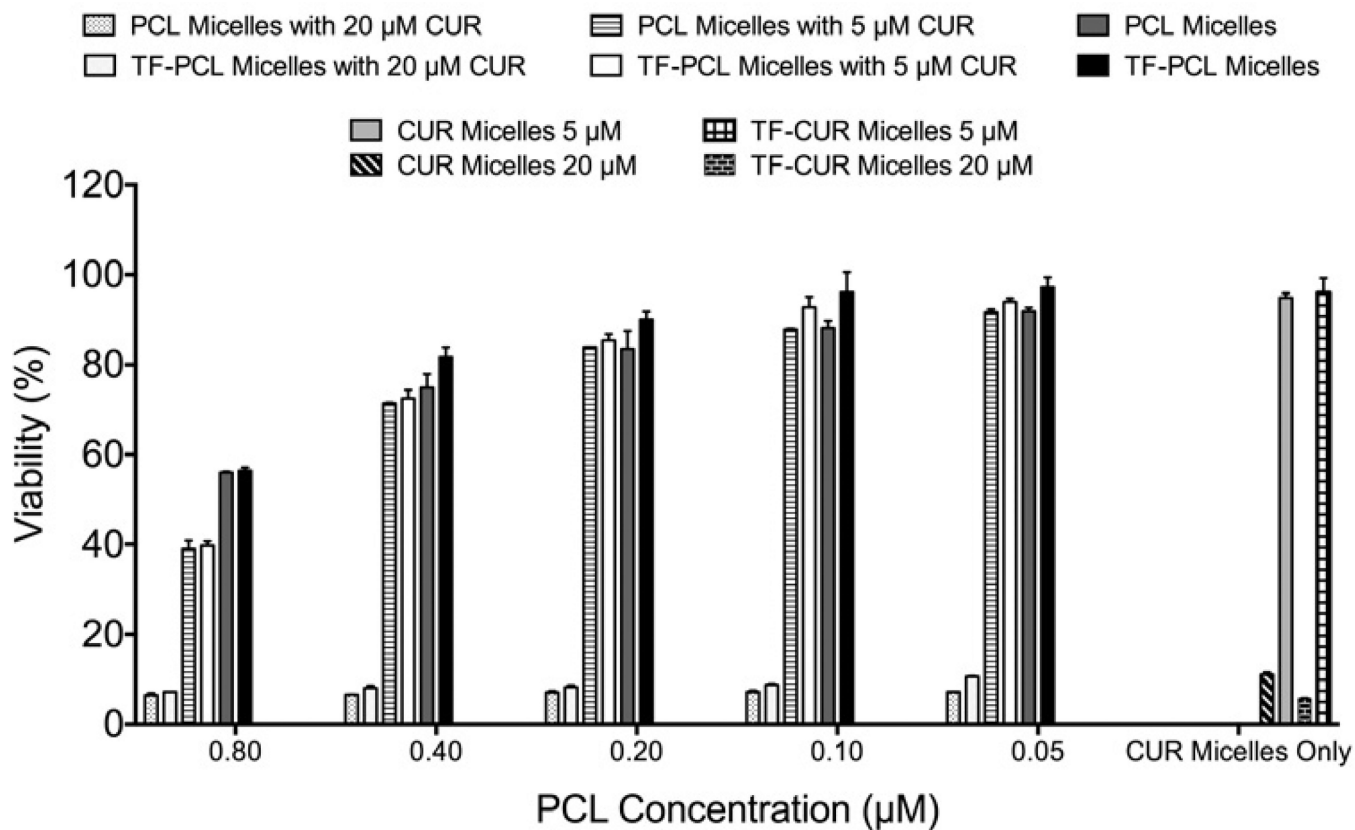


Figure 5. Cell viability of NCI-ADR-RES cell monolayers after 72 hours of continuous incubation with micelle formulations at different PCL concentration with/without CUR. Error bars indicate mean±standart deviation, n=3.

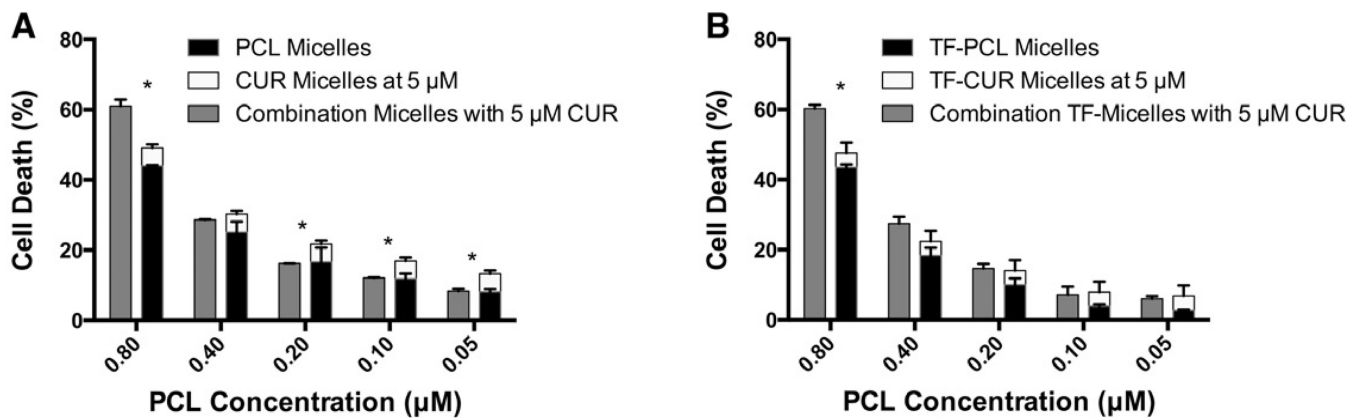


Figure 6.

Comparison of cell death of NCI-ADR-RES cells after the treatment with non-modified (A) or TF-modified (B) micellar formulations containing various concentrations of PCL, 5 μM of CUR, or combination of both.

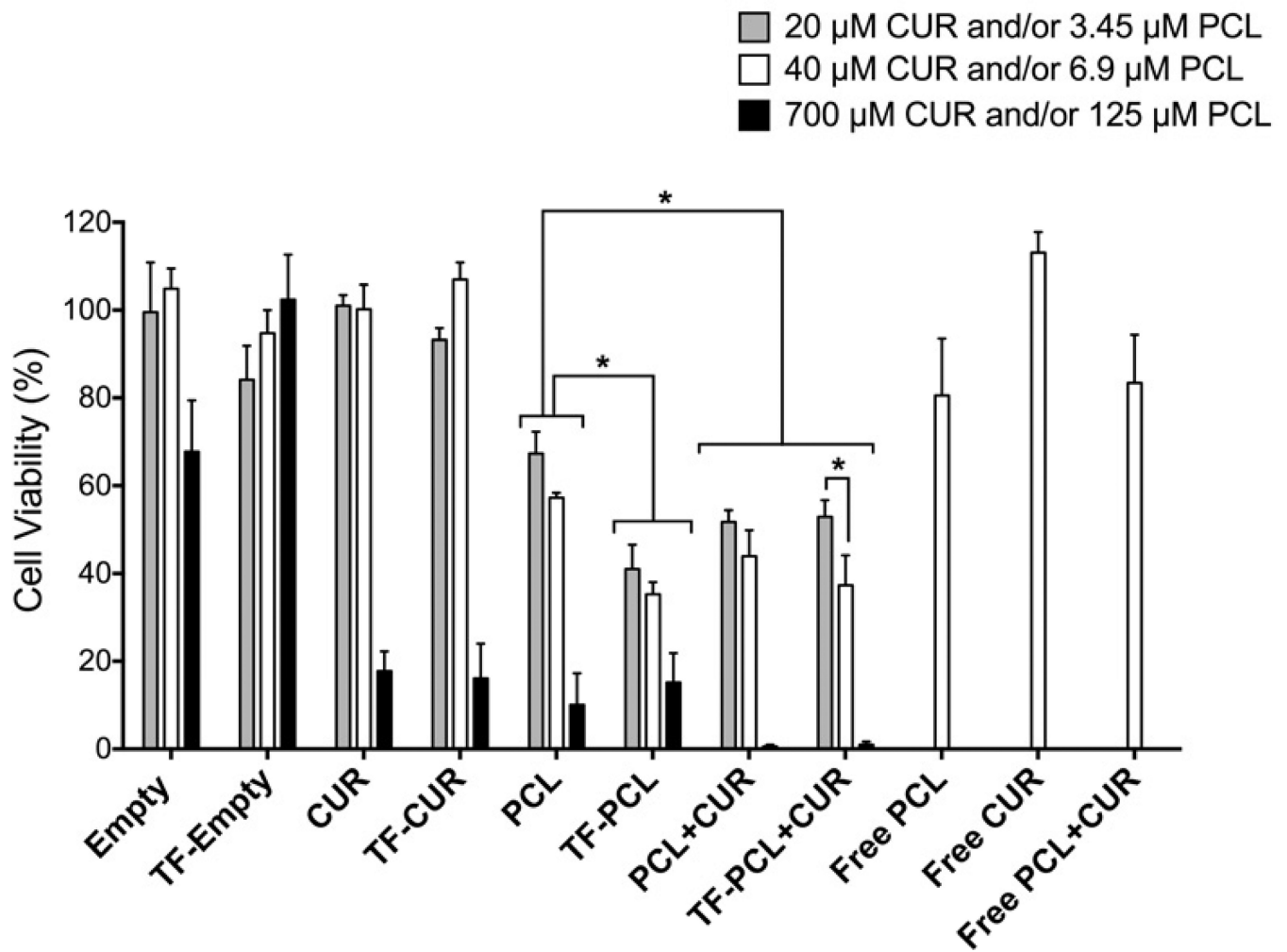


Figure 7.

Cell viability of the various formulations against NCI-ADR-RES spheroids. Five spheroids were collected as one replicate to achieve necessary sensitivity ($n=3$, 15 spheroids, mean \pm SD, * $P<0.05$).

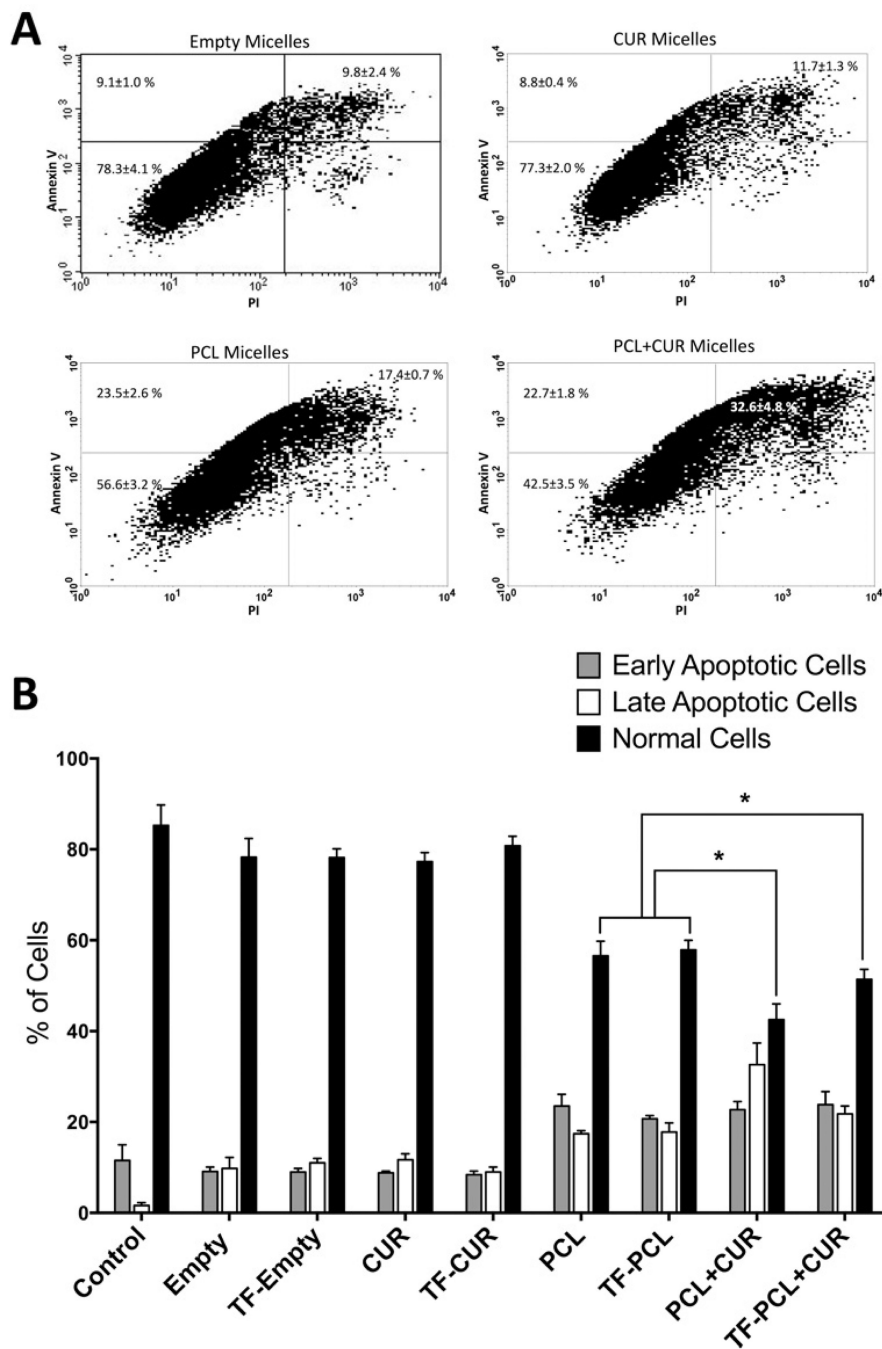


Figure 8. Apoptosis increase evaluation of spheroids after treated with different formulations. (A) Dot plot analysis results of the cells obtained from treated spheroids. Percentages of the cells corresponding to the quadrant areas were indicated in the graphs. (B) Values represent the percentage of gated 10,000 events after annexin V and propidium iodide dual staining (Error bars represent mean±SD, n=3, *P<0.05).

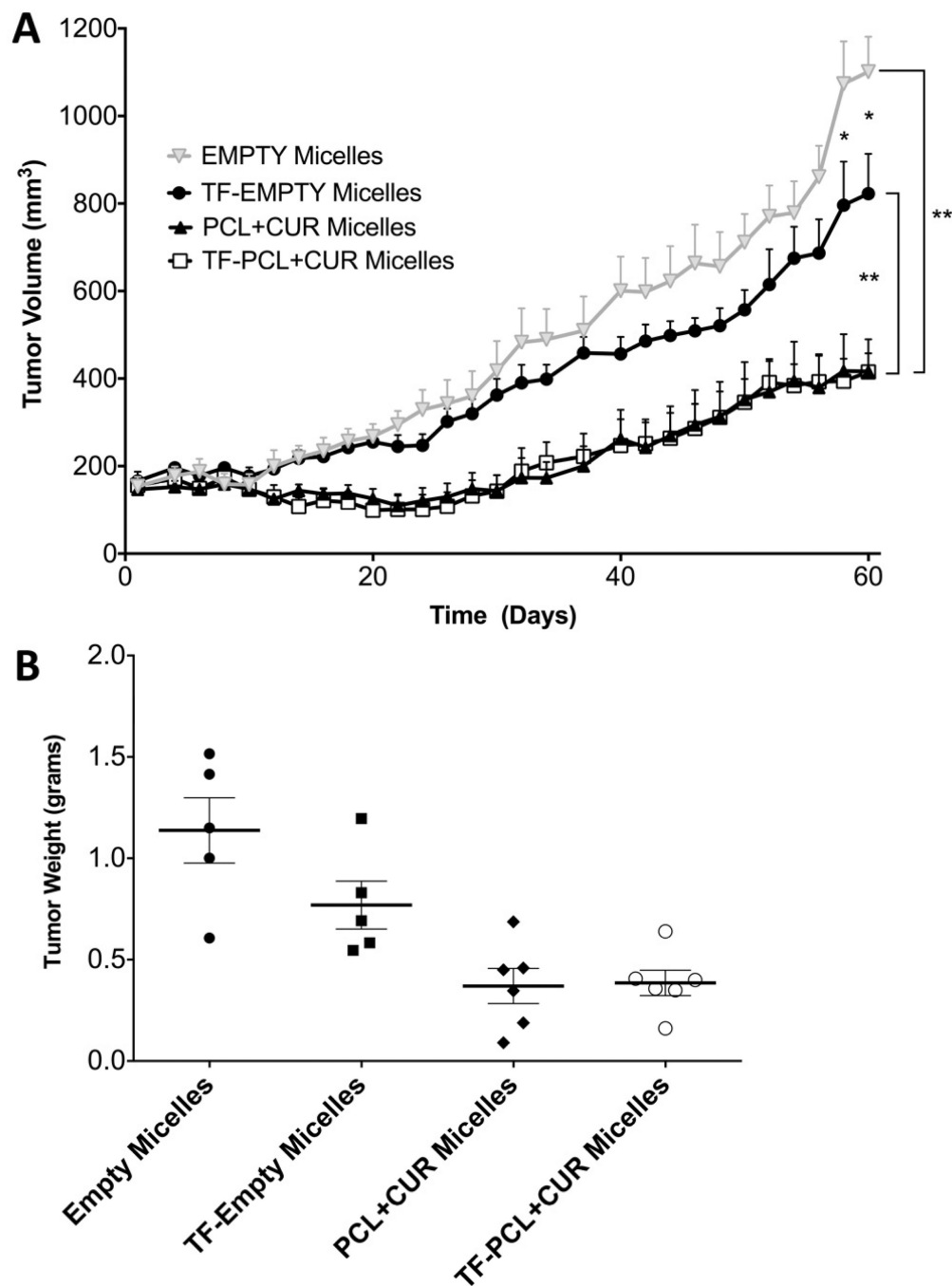


Figure 9.

In vivo studies with various micellar formulations. Nude mice bearing ~200 mm³ SK-OV-3TR tumors were treated every 3 days at a dose of 25 mg/kg CUR and 10 mg/kg PCL IP starting at day zero. Empty micelle dose was equivalent to the amount of micelle-forming material from the drug-loaded micelle groups. n = 5 per group and all values are expressed as mean ± SEM, * P < 0.01, ** P < 0.001. SK-OV-3TR tumors were harvested when the average tumor volume in the control group reached 1000 mm³ (Student's two tailed unpaired T-test,

* $P < 0.05$, $n = 5$ per group, $\text{mean} \pm \text{SEM}$). (A) Tumor inhibition study results. (B) Tumors weights at the end of the study.